Master's thesis

NTNU
Norwegian University of Science and Technology
Faculty of Natural Sciences
Department of Biology

Harini Pechiappan

Effects of Nano-and Microplastics on Inflammatory Responses in Macrophages *in vitro.*

Master's thesis in Biotechnology
Supervisor: Berit Johansen and Martin Wagner
Co-supervisor: Felicity Ashcroft
June 2021

NTNU
Norwegian University of
Science and Technology

Harini Pechiappan

Effects of Nano-and Microplastics on Inflammatory Responses in Macrophages *in vitro.*

Master's thesis in Biotechnology
Supervisor: Berit Johansen and Martin Wagner
Co-supervisor: Felicity Ashcroft
June 2021

Norwegian University of Science and Technology
Faculty of Natural Sciences
Department of Biology

NTNU
Norwegian University of
Science and Technology

Abstract

Humans can be exposed to nano-and microplastics (NMP's) *via* diet, inhalation, and possibly dermal routes, but the risk of such exposure to human health is unclear. Phagocytes are possible targets of NMP's exposure, with the potential to impact human health. Thus, the aim of this thesis was to assess if NMP exposure leads to the inflammatory activation of monocytes and macrophages. To do this, we used polydisperse secondary NMPs: polymethyl methacrylate (PMMA), polystyrene (PS), and polyvinylchloride (PVC) generated from different sources and the THP-1 cell line, undifferentiated and differentiated as a substitute for primary monocytes, and macrophages respectively.

We assessed the cytotoxicity of the NMPs in monocytes and macrophages using viability assays. After 72 h of exposure at the highest particle concentration, all three NMPs reduced the macrophage viability, whereas monocyte viability was only affected by PS. The internalization of NMP's by macrophages was determined using confocal microscopy, and we demonstrated the uptake of all three NMP types as early as 30 min after exposure. To assess pro-inflammatory responses in macrophages, we measured NF-κB translocation, expression of genes associated with M1 polarization (*CCL2, TNFα, IL-12*), and released cytokine levels (TNFα, IL-6). While stimulation with the known pro-inflammatory stimulus lipopolysaccharide (LPS) triggered NF-κB translocation, M1 macrophage polarization, and the release of TNFα and IL-6, none of the NMPs did, when given at the highest concentration for equivalent or longer time period. Exposure to NMP's during M1 macrophage polarization using IFNγ + LPS, however, suppressed TNFα release, and during M1 polarization using IFNγ alone, suppressed both TNFα and IL-6 release. In monocytes similar to macrophages, we did not observe an increase in TNFα or IL-6 in response to NMPs alone, but the exposure during LPS-stimulation suppressed TNFα and IL-6 release.

In summary, we showed that the NMPs tested were internalized by THP-1 derived macrophages yet did not trigger pro-inflammatory responses. Exposure to NMPs during pro-inflammatory stimulation of macrophages or monocytes instead inhibited cytokine release, and we thus conclude that, in certain situations, NMPs exposure could suppress immune cell activation. Given that our results in THP-1 cells contradict the effects shown in primary immune cells, the findings should

be used with caution. However, the potential for NMPs to suppress immune cell activation merits further investigation.

Acknowledgment

This master's thesis is an outcome of the two-year master's program of Biotechnology at the Norwegian University of Science and Technology (NTNU), Trondheim. The research work was conducted in the Department of Biology from November 2018 to May 2021 under the supervision of Prof. Berit Johansen via Coegin Pharma AS and NTNU.

I would like to sincerely thank my supervisor Berit Johansen for giving me this opportunity to work on this project with great encouragement, support, and guidance. I am always grateful to my co-supervisor, Felicity Ashcroft, for guiding me throughout this project, being constantly enthusiastic, supportive, and providing a generous amount of time for any help needed during this study whenever I got stuck. And also, I am incredibly thankful to the senior researcher Astrid Jullumstrø Feuerherm for her valuable guidance and cheerful words. Also, I would like to thank the rest of the PLA2 group members: Nur, Thuy, and Elisabeth, for helping in the lab and giving feedback on my work. Especially, I am grateful to my supervisor Martin Wagner for his constructive feedback, support, and encouragement throughout the project.

A special thanks to Astrid Bjørkøy from the Department of physics for teaching and helping out with confocal microscopy. Also, I would like to extend my gratitude to Stephen Gustav Kohler, from the Department of chemistry, for the training and access to Freeze-dryer. I also thank Trine Østlyng Hjertås for the training and access to the NTNU Nanolab facility and the NTA instrument.

I am thankful to many people who supported me directly or indirectly during this project. I am grateful to all my friends and lab mates for their motivation and guidance.

I would like to dedicate this thesis to my mother, Sundaravalli, who supported and motivated me with her constant love. With final mention, I thank my grandparents and father for their love and support throughout my studies.

Trondheim, 01-06-2021

Harini Pechiappan

Abbreviations

APC	Antigen-presenting cells
CLSM	Confocal laser scanning microscopy
D-PBS	Dulbecco's phosphate-buffered saline
EC20	Effective concentration 20
EFSA	European Food Safety Authority
HMC-1	Human mast cells
IC	Immune complexes
IFNγ	Interferon-gamma
LPS	Lipopolysaccharides
M-CSF	Macrophage colony-stimulating factor
MD2	Myeloid differentiation factor 2
MHC	Major histocompatibility complex
MPs	Microplastics
MPS	Mononuclear phagocyte system
MyD88	Myeloid differentiation factor 88
NF-κB	Nuclear factor-kappa B
NLRs	NOD-like receptors
NMPs	Nano- and microplastics
NPs	Nano plastics
NTA	Nano track analysis
PA	Polyamide
PBMC	Peripheral blood mononuclear cells
PBS	Phosphate buffered saline
PE	Polyethylene
PET	Polyethylene terephthalate
PMA	Phorbol 12-myristate 13-acetate
PMMA	Poly methyl methacrylate
PP	Polypropylene
PRRs	Pattern recognition receptors

PS	Polystyrene
PVC	Polyvinylchloride
ROS	Reactive oxygen species
Th-1	T helper cells 1
Th-2	T helper cells 2
TLRs	Toll-like receptors

Table of Content

1 Introduction

1.1. Microplastics – a serious issue

Plastics is one of the most prominent human-made products, pervading the earth's environment in the Anthropocene [1]. Plastic debris is becoming a major environmental concern. It is estimated that 250 million tons of plastic will accumulate in the ocean by 2025 [2]. According to Geyer and colleagues, 8.3 billion MT of virgin plastics were manufactured until 2017 [3]. If the existing manufacturing and waste disposal policies are maintained, around 12 billion tons of plastic waste would be present in landfills and nature by 2050. Consequently, plastic is a persistent environmental pollutant [3, 4]. Large quantities of plastics released into the environment accumulate and degrade into tiny micro- (1-1000 μm) [5] and nanosized (≤ 1 μm) particles [6], which are often referred to as microplastics (MP) and nano plastics (NP). Some microplastics are produced for specific applications, such as exfoliants (microbeads) in personal care products. These plastics and microfibers from machine-washed clothing are released into the environment through wastewater effluent, amongst others [7].

Polyethylene (PE), polypropylene (PP), and polystyrene (PS) are the most widely manufactured polymers, with some of them being manufactured intentionally as microplastics with particle diameters < 5mm [8]. They are referred to as primary microplastics and are mainly used in cosmetics, personal care products, and cleaning agents [9]. These fragments enter the marine world through sewage systems, surface runoff, and atmospheric deposition [10]. Environmental factors such as UV radiation, saltwater, and marine biota decompose larger plastic items disposed into the ocean, accounting for 60-80% of all plastic litter. They are known as secondary microplastics [6, 11]. The most commonly observed polymers are PE, PP > PS > PVC > polyethylene terephthalate (PET) > polyamide (PA) > polyesters, and PMMA [12].

Majorly, the primary and secondary microplastics are known to enter the food webs from the environment, and therefore humans can be exposed [13]. In general, there is a paucity of information on human susceptibility to nano-and microplastics (NMPs) and their health consequences [14]. According to the European Food Safety Authority (EFSA), information on the toxicity, toxicokinetics, and prevalence of microplastics in food is still lacking [8].

1.1.1. Microplastic exposure and human health

Humans can be exposed to microplastics via airway or gastrointestinal epithelia, and various absorption and translocation pathways, such as endocytosis and persorption, have also been identified. [15].

NMPs can enter the human body through three main routes: internalization, inhalation, and dermal uptake [16]. NMPs having a particle size ≤ of 6 μm can move through the intestinal wall of rodents and translocate into the lymphoid system, resulting in lymph node contact [17]. In the lungs, the NMPs are phagocytized by resident macrophages of the innate immune system, as often they get trapped in the pulmonary mucous [18]. The NMPs ingested by the macrophages are eliminated from the lung by mucociliary processes or transported to lymph nodes when ≤ 7 μm [18, 19]. Although NMP absorption through the skin appears to be limited, some studies have reported that NMPs having a particle size of ≤ 500 nm can enter *via* hair follicles and get transported to lymph nodes [20, 21]. From lymph nodes, NMP (< 7 μm) can be transported to the spleen, liver, and kidneys through the circulatory system [22, 23]. NMPs can interact with various immune cells in the process, including lymphocytes (T cells and B cells), monocytes, dendritic cells, macrophages, and neutrophilic granulocytes [24].

The effects of microplastics are less well-understood than their distribution and retention in the human body. However, some preliminary studies have shown a few potentially harmful effects, including elevated inflammatory responses, size-related toxicity of plastic particles, chemical transmission from adsorbed chemical compounds, and degradation of the gut microbiome [7]. Physical properties of these particles such as size, shape, surface charge, functional groups, buoyancy, and hydrophobicity can influence the absorption of the microplastics [25, 26]

The potential for the immune system to respond to NMP exposure can be investigated in macrophages. Macrophages are an essential part of the innate immune system, as they are responsible for detecting and removing foreign objects that pass through the epithelial barrier. As this happens, intestinal macrophages engage in respiratory burst action, triggering pro-or anti-inflammatory responses and releasing inflammatory cytokines.

1.2. Monocytes and macrophages – key players of the innate immune system

The innate immune system is the primary line of defense invading against pathogens and comprises various mechanisms from physical barriers to cellular components. After recognizing a pathogen, the innate system activates a broad immune response [27] consisting of a collection of effector cells: phagocytic, epithelial, and endothelial cells, natural killer cells, innate lymphoid cells, and platelets to prevent infection.

Phagocytic cells include monocytes, dendritic cells, macrophages, and granulocytes (i.e., eosinophils, neutrophils, basophils, and mast cells) [28]. In response to inflammation, the mononuclear phagocyte system (MPS) represents a set of leukocytes, circulating in the blood as monocytes and residing in the tissues as macrophages [29].

1.2.1. Monocytes

Monocytes are leukocytes that originate in the bone marrow and circulate in the spleen and blood. They are immune effector cells armed with chemokine receptors and pattern recognition receptors (PRRs), which enable them to recognize "danger signals" and migrate from blood to tissues to help the elimination of infection [30]. However, in response to infection and injury, monocytes can proliferate. The functions of monocytes include phagocytosis and antigen presentation, chemokine secretion, and after being recruited to tissues, monocytes can differentiate into both macrophages and dendritic cells [31].

Monocytes have a variety of receptors that monitor and sense changes in the environment. They are highly plastic and heterogeneous, and as they come into contact with a foreign body, they alter their functional phenotype by differentiating as inflammatory or anti-inflammatory sub-types [32].

In recent studies, human monocytes are classified into three subsets by the expression of surface markers CD16 and CD14 [33]. The classification of these subsets and their particular functions in homeostasis and inflammation is not well defined. About 80-90% are commonly known as “classical monocytes,” which express significant levels of CD14, lack surface expression of CD16, and are phagocytic with no inflammatory characteristics [34]. The rest 10-20% of human monocytes are divided into two subtypes: “non-classical monocytes” which are more abundant, exhibiting low surface CD14 expression but high CD16 levels and showing inflammatory

characteristics, and “intermediate monocytes” which have a high-level expression of both CD14 and CD16 surface markers [33, 35].

1.2.2. Macrophages

Macrophages are native phagocytic cells found in both lymphoid and non-lymphoid tissues. They have a wide range of pathogen-recognizing receptors, which participate in phagocytosis and activation of inflammatory cytokine production. They are considered essential in steady-state tissue homeostasis for the growth factor production and clearance of apoptotic cells [36]. Unlike monocytes, macrophages are terminally differentiated cells but have similar functions, contributing to the phagocytosis of pathogens and toxins, and chemokines secretion for recruiting other immune cells. In addition, macrophages can act as antigen-presenting cells (APC) [37], migrating via the lymphatics to the lymph nodes for presenting the processed antigen [31].

Activation of macrophages occurs in two ways. The first is known as “classical” or “M1” activation, which results in a pro-inflammatory phenotype. In response to extracellular or intracellular pathogens through PRRs, M1 macrophages up-regulate inducible nitric oxide synthase and secrete pro-inflammatory chemokines and cytokines. They often use MHC class II to present antigen, which leads to inflammation, granulocyte recruitment, and a Type-1 helper (Th-1) T cell response [31]. The “alternative” or “M2” activation is more diverse. M2 macrophages secrete histamine in response to IL-4 and IL-13 during an allergic response or parasitic infection, promoting killing and encapsulation of parasites and a Type-2 helper (Th-2) T cell response [38]. These macrophages can down-regulate the initial inflammatory response and promote inflammatory resolution, activating the tissue healing and fibrosis beyond the domain of the pathogen response. Thus, M2 activation is also known as an anti-inflammatory phenotype [39].

Notably, the characterization of M1/M2 activation classification is likely too binary. The macrophage activation states are defined better in response to various stimuli, with responses varying from pro-inflammatory to anti-inflammatory [40].

Upon pathogen recognition by the innate immune receptors and activation of macrophages, a signal is generated to communicate with the nucleus. This signal results in the elevated expression of adhesion molecules and cytokines, which depends on the activation of several inducible transcription factors, such as nuclear factor-kappa B (NF-κB) [41]. It plays a significant role in

regulating gene transcription, which is involved in inflammatory responses, mainly pro-inflammatory [42, 43].

1.3. THP-1 cell line – a human monocyte *in vitro* model

THP-1 is a human leukemic monocytic cell line isolated from the peripheral blood of a one-year-old boy who suffered from acute monocytic leukemia [44] that has been broadly used to study monocyte and macrophage biology. According to early research, THP-1 cells have morphological and functional properties similar to primary monocytes and macrophages, including macrophage differentiation markers [45, 46]. When THP-1 macrophages are stimulated with lipopolysaccharide (LPS), they express CD14, MD2, and MyD88 genes, which are necessary for LPS signaling *in vivo* [47]. This cell line has been a standard model for predicting the monocyte and macrophage behavior [48].

Advantages of using THP-1 cells over primary monocytes include a high growth rate, low risk of viral infections, and sustaining with the same characteristics for 3 months. Furthermore, the cells have a homogeneous genetic inheritance, reducing the degree of variability in the cells' phenotype [48].

In many experiments, LPS is used to simulate bacterial infection in THP-1 cells. Like primary macrophages, the cells can polarize, inducing a change in gene expression and the release of cytokines such as TNFα, IL-10, IL-1β, IL-6, and IL-8 in response to LPS. The effects of medications and natural products on macrophage function have been studied using this method [49].

1.4. Differentiation of THP-1 monocytes to macrophages

Cell adherence, high phagocytic behavior, and expression of dependent cell surface markers such as CD14, CD36, CR3 (CD11b/CD18), and TLR-2 can all be used to regulate THP-1 macrophage differentiation [48].

Treatment with phorbol-12-myristate-13-acetate (PMA), 1,25-dihydroxyvitamin D3 (vD3, also known as calcitriol), or macrophage colony-stimulating factor (M-CSF) have all been used to successfully differentiate THP-1 cells from monocytes to macrophages [48, 50, 51]. However, M-CSF is known to work better for differentiating the early monoblasts into monocytes before their release into the peripheral blood. As a result, it is more commonly used for the *in vitro* differentiation of bone marrow-derived monocytes into macrophages [52, 53].

PMA is shown to be the most effective differentiation agent for obtaining mature THP-1 monocyte-derived macrophages, similar to peripheral blood mononuclear cell (PBMC) monocyte-derived macrophages [34, 35] (Figure 1.1). Following stimulation with PMA, THP-1 cells may develop macrophage characteristics: they adhere to culture plates, change their morphology to flat and amoeboid in shape with developed Golgi apparatuses, rough endoplasmic reticula, and large numbers of ribosomes in the cytoplasm [46].

Other studies have determined that a concentration of 100 ng/ml PMA was sufficient for complete differentiation of THP-1 monocytes to macrophages and that higher PMA concentrations may trigger undesirable responses, especially responses derived from the activation of NF-κB [49].

Additionally, it was shown that resting the differentiated macrophages in culture media without PMA for at least 24 h increased the expression of macrophage-specific marker genes and decreased NF-κB gene clusters that were up-regulated during the PMA-induced differentiation [47]. Daigneault et al. demonstrated that differentiation with 200 nM PMA for 3 d followed by 5 d in culture media with no PMA increased the macrophage markers expression, including differentiation-dependent cell surface markers with a comparable pattern PBMC-monocyte related macrophages [50].

THP-1 cells differentiated using 100 nM vD3 for 3 d were shown to be less comparable to PBMC monocyte-derived macrophages in terms of phagocytic activity and production of IL-1β and TNFα than THP-1 macrophages differentiated with 200 nM PMA for 3 d [50, 54].

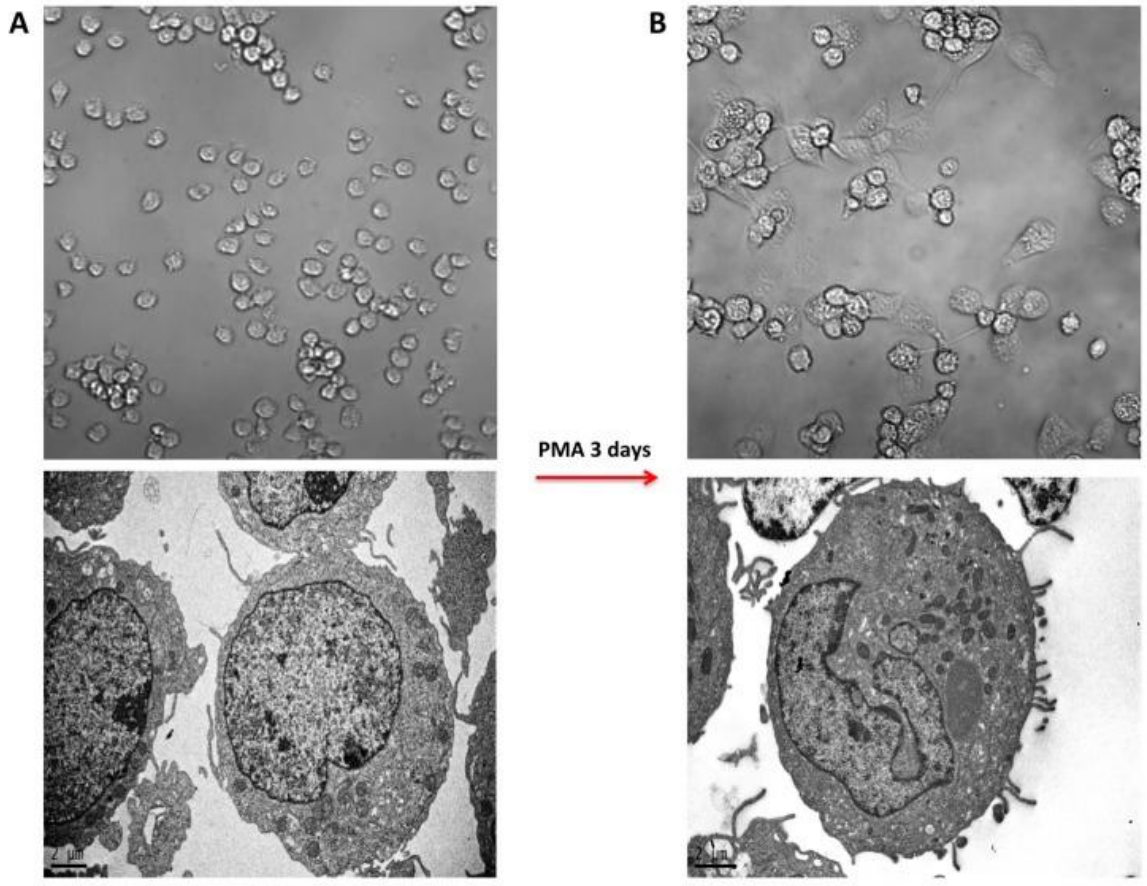

Figure 1.1. Differentiation of THP-1 monocytes into macrophages using PMA for 3 d. The monocytes show well-developed and structured organelles with greater adherence. The image shows **(a)** undifferentiated and **(b)** differentiated THP-1 cells with morphological changes induced by PMA treatment. This image is obtained using optical and transmission electron microscopy. Figure from Francesca Gatto et al. [55]

1.5. Polarization of macrophages

In vivo, macrophages are plastic and heterogeneous cells, which polarize differentially in response to specific stimuli and tissue localization. Different CD^{4+} T cell subsets, among other cell types, are essential regulators of macrophage differentiation into different phenotypes *in vivo*. Interferon-gamma (IFNγ) stimulation produces M1 macrophages, which are classically activated, while stimulation with IL-4, IL-13, and IL-10 produces M2 macrophages, which are alternatively activated (Figure 1.2) [56-58].

Characterization of differential phenotypes is understood based on observations that M1 macrophages play a role in producing pro-inflammatory cytokines production and provide host defense against microbes and promote tumor regression [59] by triggering a Th1-driven immune response [60]. During M1 activation, the expression of TNFα, IL-6, IL-8, IL-1β, and IL-12 genes, as well as PRRs like NOD-like receptors (NLRs) and Toll-like receptors (TLRs), is up-regulated [56]. Alternatively, M2-type macrophages stimulate a Th2-driven immune response [40], which aids in resolving parasite infections, tissue modeling, immune modulation, allergy, and tumor progression [61]. The M2 activation is characterized by the release of anti-inflammatory cytokines IL-10, CCL1, CCL22, CCL16, CCL17, CCL18, and CCL24 and expression of arginase-1 mannose scavenger receptors [62].

M2 macrophages are categorized into three subsets: M2a, which is induced by IL-4 or IL-13; M2b, induced by immune complexes (IC)/TLR-agonists or IL-1 receptor; and M2c, which is induced by IL-10 [62]. Mantovani et al. proposed that these M2 subtype traits are linked to particular roles such as pathogen destruction, immune modulation, and tissue remodeling [62]

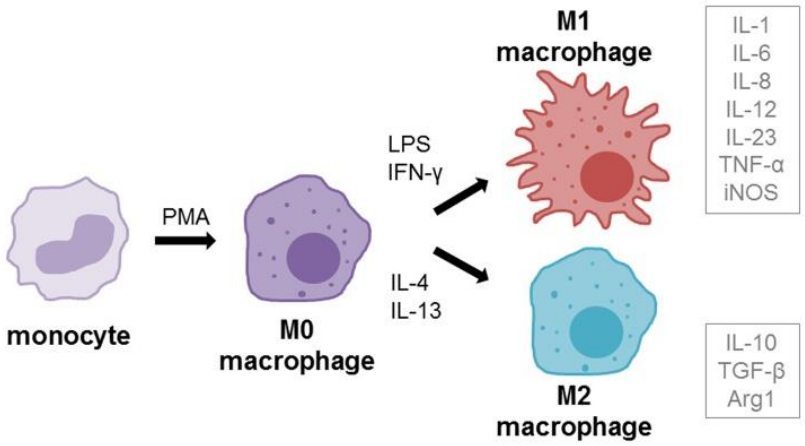

Figure 1.2. Differentiation and Polarization of Macrophages *in vitro*. Monocytes can be differentiated into macrophages using the differentiation agent PMA. LPS and IFNγ can further polarize macrophages into the M1 (pro-inflammatory, classically activated) phenotype, or IL-4 and IL-13 can polarize them into the M2 (anti-inflammatory, alternatively activated) phenotype. Grey boxes next to the polarization phenotypes indicate the cytokines that are primarily secreted by each phenotype. Figure from Bezold et al. [63]

The polarization of THP-1 cells for *in vitro* studies was described by Chanput et al., as PMA-differentiated macrophages were treated with 20 ng/ml IFNγ + 1 μg/ml LPS for 6 h for M1 phenotype and 20 ng/ml IL-14 for 24 h for M2 phenotype. Various well-established markers of

the M1 and M2 phenotypes were found to be up-regulated during the THP-1 macrophage polarization. It was shown that TNF-α, IL-12p40, IL-6, IL-1β, and IL-8 can be used as M1 marker genes, and MRC-1, TGFβ-1, SOCS1, PPARγ can be used as M2 marker genes [49, 64].

1.6. The toxicity and immune response to NMP's in human cells

Various toxicological studies with NMP's have been carried out *in vitro* for investigating the behavior and effects of NMP's [65]. Accordingly, NMPs are most often implicated in the development of neurotoxicity, cytotoxicity, and oxidative stress [12]. These studies point towards oxidative stress and inflammatory responses as key factors of NMP toxicity [16, 66].

Surprisingly, although demonstrating a degree of cellular absorption, studies found no or minor evidence of cellular toxicity even at extremely high NMP concentrations [13, 67, 68].

As mentioned previously, human exposure routes for NMP's include internalization and inhalation [16]. Accordingly, studies in various epithelial cell line models have been reported - Polyethylene terephthalate (PET) NPs produced by laser ablation were tested on the Caco-2 human gut adenocarcinoma epithelial line; the researchers discovered a tendency for NMP uptake and transcellular transport across a Caco-2 cells-based intestinal barrier model [67].

Studies in BEAS-2B, human lung epithelial cells by Dong and colleagues showed that PS MPs caused cytotoxicity, inflammatory responses, and oxidative stress in human lung epithelial cells and disrupted the epithelial cell layer, at least *in vitro* [69]. In the A549 human alveolar epithelial line, Xu and co-workers discovered that PS NPs (25 and 70 nm) reduced cell viability, caused cell cycle arrest, and up-regulated nuclear factor NF-κB along with some pro-inflammatory cytokines [70].

Prietl and co-workers demonstrated that 20 nm carboxylated PS NMPs are readily absorbed by human monocytic cells and are cytotoxic. Larger NMPs (500 and 1000 nm) induced the secretion of cytokines, including IL-8 and IL-6, from monocytes and macrophages, as well as a detectable degree of respiratory burst in monocytes [66].

Hwang et al. showed cytotoxicity and ROS induction associated with exposure to high concentrations of 20 μm polypropylene (PP) MPs using PBMCs, Raw 264.7 (murine macrophages), and HMC-1 (mast cells). The MPs also increased the release of histamine from mast cell lines and mediated pro-inflammatory cytokines IL-6 and TNFα from PBMCs [71].

The inflammatory response to exposure of irregular PMMA, PVC, PS plastic particles, and PS nanospheres was investigated in primary human monocytes and dendritic cells (Weber et al. unpublished). Elevated concentrations of TNFα, IL-6, and IL-10 were seen in both cell types following the exposure to irregular PVC.

Overall, ROS production and expression of inflammatory cytokines appear to be common responses of human cells exposed to various NMPs.

2 The rationale of the study

As part of the innate immune system, monocytes and macrophages ingest pathogens and other foreign particles that enter the body. To gain a better understanding of the potential risks that NMP exposures pose to human health, ongoing research has been aimed at determining how the immune system responds to interactions with these particles. Specifically, exposure to certain polydisperse NMPs was shown to trigger the release of cytokines from primary human monocytes and dendritic cells (Weber et al. unpublished).

The aim of this thesis was to further study how the human immune system interacts with secondary NMPs by the following specific goals:

1. Producing and characterizing (concentration and size distribution) a set of polydisperse NMPs representing three common polymer types (PMMA, PS, PVC)

2. Investigating the cytotoxic effects of NMP exposure in monocytes and macrophages using a human monocytic cell model (THP-1)

3. Determining whether NMPs are ingested by THP-1 derived macrophages using confocal laser scanning microscopy

4. Assessing inflammatory responses to NMP exposure in THP-1 derived macrophages by measuring (i) activation of NF-κB, (ii) expression of genes associated with macrophage polarization, and (iii) the release of cytokines

5. Assessing inflammatory responses to NMP exposure in THP-1 monocytes by measuring cytokine release

3 Materials and methods

3.1. Materials

Unless otherwise mentioned, all chemicals were purchased from Sigma-Aldrich. For quantitative PCR, Sigma- Aldrich's KiCqStart® and SYBR® Green Primers were used.

3.2. Preparation of NMP's

The polydisperse PMMA (green fluorescent) and PS particles (orange fluorescent) were generated by cryomilling household materials. PyroPowders (Erfurt, Germany) provided irregular PVC powder (non-fluorescent) (<50µm) with a nominal particle size range of 13-17 µm. The milled plastics samples were provided by Prof. Martin Wagner, NTNU, Norway. To separate particles with sizes ≤ 5 µm, we suspended 15–35 mg of plastic powder in 1 ml of ultrapure water (15 × 1.5 ml tubes per NMP type). After the suspensions were sonicated at room temperature for 1 h, they were allowed to settle for 24 min (PS, PMMA) and 12 min (PVC) at room temperature. This step was performed to allow particles with sizes > 5 µm to settle. The settling times used were calculated using Stoke's Law. PS particles > 5 µm had a theoretical settling time of 114 min. The time was shortened to 24 min because the particles did not settle but rather adsorbed to the surface of the tubes.

After settling, 750 µl of supernatant from each tube was pooled together, frozen at -20°C, and lyophilized overnight to concentrate the NMP suspensions. The resulting plastic powders were resuspended in 1 ml PBS for PVC and PMMA, whereas the PS was resuspended in PBS containing 1:10,000 diluted surfactant (Tween® 20) to avoid agglomeration.

From the 1ml plastic suspension concentrates, a working stock of 1:5 dilution was prepared in PBS for the experiments. For vehicle controls, we used PBS without plastics for PVC and PMMA and PBS with Tween® 20 (1:10,000) for PS.

3.3. Nanoparticle tracking analysis of particle size distribution and concentration

Nanoparticle tracking analysis (NTA) with a NanoSight LM10 (Malvern Panalytical, Netherlands/United Kingdom) was used to assess suspended particle concentrations and size distributions. As NTA requires a concentration of $10^6 – 10^9$ particles/ml, all the suspensions were

diluted with ultrapure water [72]. We prepared the same dilutions of the plastic-free control with the same dilution factor for each dilution to obtain comparable control measurements. For PS control, the dilution was prepared with PBS + 1:10,000 Tween® 20. For each dilution, three replicates were prepared, and we took three repeated measurements for each replicate. The video recording time was set to 60 s. The captures were repeated in the videos with < 200 valid particle counts, and the time was increased to 120 s. The measurements were taken using a CCD camera with a red laser (638 nm). Detailed settings of NTA used for measurements of the particle stock suspensions are shown in Appendix B.1.

By subtracting the particle concentration in the corresponding particle-free control, particle concentrations in the stock suspensions were blank-corrected.

The NTA analysis provides the concentration in particles/ml, the size of individual particles, and the mean and median (D50) of the particle size for the samples. The size distribution of the NMPs is presented as the relative particle abundance (RPA) fit to a lognormal distribution using GraphPad Prism (version 9.01, San Diego, CA).

Final particle concentrations (particles/ml) are the average of three replicates for each NMP.

3.4. Measurement of particle size distribution and settling time using time-lapse microscopy

Particle settling times, including the size distribution of the settled particles, was measured by time-lapse microscopy using a confocal laser scanning microscope (CLSM) (Zeiss LSM 800)

An 8-well chambered coverglass (Nunc™ Lab-Tek™ II; Cat no.155409) filled with 300 µl of media was placed on the stage. The particles were diluted with PBS (1:3) from the working stock, and 30 µl of NMP was added to the media. After the addition of the particles, the time-lapse recording was started. The non-fluorescent PVC particles were stained with Nile Red (1:40 dilution) before the addition.

A series of z-stacks were taken at 15 min intervals for 45 cycles (PMMA), 63 cycles (PS), and 50 cycles (PVC). The imaging settings used to visualize the fluorescent plastic particles are shown in Appendix B.2.

The captured images were analyzed using the CellProfiler software [73] with the help of my co-supervisor. CellProfiler data were used to plot the size distribution of the settled particles and the time taken for the particles of a given size to settle. The size distribution is presented as RPA fit to a Lognormal distribution using Graphpad prism as mentioned in 3.2.

3.5. Cell culture

3.5.1. Maintenance of THP-1 cells

Human monocytic THP-1 cells (ATCC, Manassas, VA, USA) were cultivated in RPMI 1640 medium supplemented with 10% fetal bovine serum (FBS), 5ml L-glutamine, 1ml gentamycin, and 0.05mM 2-β-mercaptoethanol. The cells were incubated at 37 °C in a humidified environment of 5% CO_2 in a T-75cm^2 culture flask. The growth medium was replaced every 4-5 days by diluting cell suspension to a cell density of 2×10^5 cells/ml to prevent the cell density from reaching more than 1×10^6 cells/ml as high cell density can create a stressful environment. Maintaining the logarithmic growth phase of the cells is essential to keep them healthy. The cells were allowed to grow for one week after being thawed from -80 ^oC, and the cells were used for experiments between passages 10 and 24.

3.5.2. Optimization of the differentiation of THP-1 monocytes to macrophages

We previously optimized the protocol to differentiate THP-1 monocytes to macrophages under the Biotechnology Specialization project (TBT4500) course. Briefly, THP-1 cells were plated at a density of 1×10^6 cells/ml and treated with 10 nM PMA for either 24 h or 48 h. Quantitative PCR analysis showed that the expression levels of macrophage surface markers CD14 and CD36 were up-regulated after 24 h (results shown in Appendix C). Thus, the differentiation of THP-1 monocytes into macrophages was carried out by the addition of 10 nM PMA for 24 h.

To further optimize this protocol, after the 24 h of PMA treatment, the media was changed to allow the differentiated cells to rest for different lengths of time (1, 2, 3, 5 d) before M1 stimulation using 20 ng/ml IFNγ along with LPS concentrations (100 ng/ml or10 pg/ml) for 16 h. RNA was extracted for qPCR analysis of polarization specific marker genes, and 2 d rest was decided to be optimal; thus, unless otherwise stated, THP-1 derived macrophages were differentiated by treatment with PMA (10 nM for 24 h) followed by media replacement and resting the cells for 2 d.

3.6. Exposure of THP-1 cells to NMPs

THP-1 cells were seeded in 12-well plates at density 1×10^6 cells/ml, and the following exposure conditions were performed.

1. Directly exposed to different NMPs for 18 h.
2. Stimulated with 300 pg/ml LPS (effective concentration 20) (EC20) in combination with the NMP samples for 18 h.
3. Differentiated into macrophages and exposed to NMPs for 16 h.
4. Differentiated macrophages were exposed to NMPs during polarization into an M1 phenotype using a combination of 20 ng/ml IFNγ and 20 pg/ml LPS (EC20) for 16 h.

We added 50 µl of plastic particles to 1ml of media, resulting in a final concentration of 9.10×10^8 (PMMA), 8.82×10^7 (PS), and 5.84×10^9 (PVC) particles/ml. Theoretical concentrations were calculated using the concentrations in particles/ml, density, and the average size of the NMPs, by assuming the polydisperse particles as spheres. The estimated concentrations were 3.7 µg/ml (PMMA), 0.3 µg/ml (PS) and 4.2 mg/ml (PVC).

The cell pellets were collected by centrifugation at 2000 rpm for 10 min at 4°C, and adherent cells were scraped for combined lysis in Buffer RLT from the RNA isolation kit. The supernatant was collected for cytokine analysis by ELISA. Supernatants and lysed cell pellets were stored at -80°C.

3.7. Cytotoxicity assay (Resazurin assay)

Cells were seeded into 96 well plates at a density of 1×10^4 cells/90 µl. The outer wells of the plate were filled with 200 µl of phosphate buffer saline (PBS) to prevent any edge effects. To test for cytotoxicity in monocytes, the cells were directly treated with NMPs for 24 h or 72 h before the resazurin assay.

To test for cytotoxicity in macrophages, the THP-1 cells were first differentiated to macrophages before NMPs were added and incubated for 24 h or 72 h.

For treatments, a 1:3 serial dilution of each polymer type was prepared in PBS (PVC and PMMA) or PBS +1:10,000 Tween® 20 (PS), and 10 µl was added to 90 µl media per well of the 96 well plates. Treatments were performed using 3 technical replicates, and the data shown represent 3

independent experiments. Table 3.1 shows the final particle concentrations (in µg/ml and mg/ml) that the cells were exposed to in the cytotoxicity studies.

Table 3.1. Theoretical concentrations of NMP's used in the cytotoxicity experiment with THP-1 cells

Dilutions	PVC (mg/ml)	PMMA (µg/ml)	PS (µg/ml)
1	25.400	22	1.520
2	8.467	7.333	0.507
3	2.822	2.444	0.169
4	0.941	0.815	0.056
5	0.314	0.272	0.019
6	0.105	0.091	0.006
7	0.035	0.030	0.002
8	0.012	0.010	0.001
9	0.004	0.003	0.000

The use of the non-toxic redox dye resazurin is a common technique for determining cell viability. The cells with active metabolism form a pink fluorescent resorufin product by the resazurin compound's reduction. The fluorescence emitted is directly proportional to the viable cell count [74].

10 µl/well of the resazurin reagent was added to each well, followed by 2 h incubation. The fluorescence was measured using the Cytation^{TM} 5 Cell Imaging Multi-Mode Reader (Biotek Instruments Inc.) at 544 nm excitation and 590 nm emission.

3.8. Cellular uptake of NMPs in THP-1 derived macrophages

THP-1 cells were plated at a concentration of 1×10^4 cells in 500 µl media in an 8-well chambered coverglass and differentiated into macrophages. The cells were treated with 25 µl of NMP for either 30 min or 16 h, resulting in cells being exposed to the following final particle concentrations: 9.10×10^8 (PMMA), 8.82×10^7 (PS), and 5.84×10^9 (PVC) particles/well. The cells were stained as described below to visualize the plasma membrane. We imaged the cells and fluorescent particles using laser scanning confocal microscopy to determine whether the particles had been internalized.

3.8.1. Staining of PVC plastic particles with Nile Red

As the PVC was non-fluorescent, we stained the particles using Nile Red, as was previously described [75]. Nile Red stain was added to the PVC particles at a concentration of 1:40 dilution and incubated for 8-10 min at room temperature. The tube was then centrifuged at high speed (15,000 rpm) for 5 min, forming a pellet of the stained PVC particles. After discarding the supernatant, the stained PVC pellet was suspended again in the same volume of PBS and used for treatments. To control for residual or leached Nile Red staining of lipid in the cells, we previously resuspended a second stained PVC pellet in culture media and stored it for 16 h. After this, the particles were again centrifuged (15,000 rpm, 5 min), and the supernatant was given to the cells.

3.8.2. Plasma membrane staining and CLSM

Following treatment with NMPs, the cells were washed twice with 1X Dulbecco's phosphate-buffered saline (D-PBS) followed by the addition of CellMask™ Deep red plasma membrane stain (Invitrogen) (1:1000 dilution) for 5-10 min at 37°C. The cells were washed twice with D-PBS and then imaged immediately using a Zeiss LSM800 with 63x/1.4 oil immersion objective. Z-stacks were taken with a pinhole diameter equivalent to 1 Airy unit, and 4 frames were averaged per image. Laser and detection settings are shown in Table 3.2.

Table 3.2. Settings for the Zeiss LSM 800

NMP/filter	Excitation	Emission
CellMask (A-647)	640 nm	668 nm
PMMA (FITC)	488 nm	519 nm
PS (AF546)	561 nm	572 nm
PVC (Nile Red)	561 nm	636 nm

3.9. NF-κB translocation assay

3.9.1. Principle of the assay

This assay is to measure Nuclear Factor kappa B (NF-κB) translocation from cytoplasm to the nucleus. NF-κB represents a family of transcription factors, helps regulate the inducible expression of genes involved in the immune responses [76]. NF-κB, being most abundant in the immune cells, exists either as a homodimer p65/p65 or heterodimer p65/rel A and p50 in the cytoplasm. The NF-

κB transcription factor's function is promoted by the p65 component, containing the primary transactivating domain. An inhibitory molecule, IκBα associating with cytoplasmic sequestration, helps in regulating the NF-κB activity.

Due to intracellular signaling cascades induced by various stimulants like LPS, IκBα gets phosphorylated, which leads to self-degradation, activating the NF-κB, which allows the translocation of p65/rel A from the cytoplasm. After entering the nucleus, NF-κB binds to specific sites in the TNFα promoter, activating gene transcription of TNFα. An overview of NF-κB activation and translocation into the nucleus in THP-1 cells and PMA-differentiated macrophages with TNFα secretion can be seen in Figure 3.1 [77].

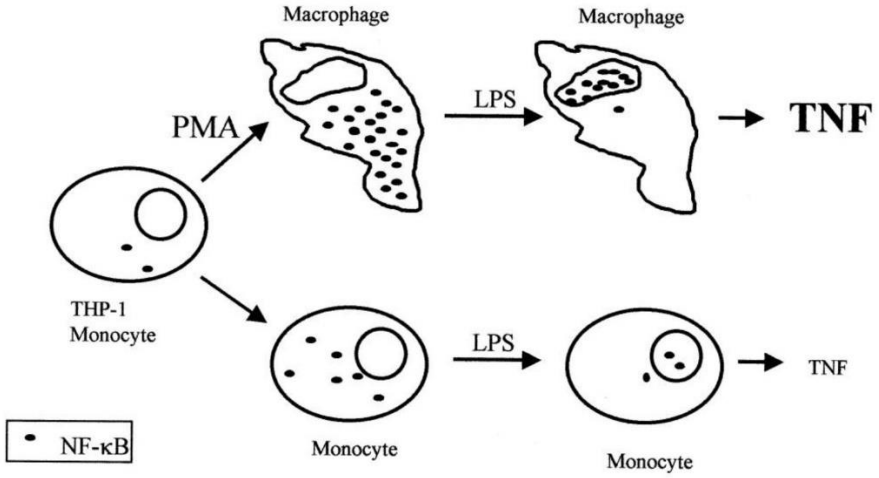

Figure 3.1. The relationship between monocyte differentiation, NF-κB translocation, and TNFα secretion. Monocytes (THP-1 cells) differentiate into macrophages when treated with PMA, promoting the accumulation of NF-κB in the cytoplasm. Translocation of NF-κB is induced upon LPS stimulation resulting in TNFα secretion. Undifferentiated THP-1 cells have lower levels of NF-κB and secrete less TNFα in response to LPS stimulation, compared to the macrophages. Figure from Takashiba et al. [77]

The translocation of the activated NF-κB from the cytoplasm to the nucleus can be imaged by immunofluorescence staining. Images captured can be quantitatively analyzed using image processing software [78].

3.9.2. Optimization of the assay

THP-1 cells were seeded at a density of 10,000 cells/well in a 96-well black flat optical-bottom plate (Thermo Scientific^{TM} Nunc MicroWell) and treated with PMA (10nM) for 24 h. The media was changed, and the differentiated cells were allowed to rest for either 2 or 5 d. After resting, the

cells were stimulated by the addition of LPS (100 ng/ml) and incubated for various times (15 min, 30 min, 1-, 2-, 3- and 6 h) before being fixed and immuno-stained, as described below.

3.9.3. Exposure to NMPs

THP-1 cells were seeded at a density of 10,000 cells/well in a 96-well black flat optical-bottom plate (Thermo Scientific™ Nunc MicroWell) and treated with PMA (10nM) for 24 h. The media was changed, and the differentiated cells were allowed to rest for 2 days before treatment with NMPs for various time-points (15 min, 30 min, 1-, 2-, 3-, 6-, 8-, 16- and 24 h) before fixation and immunostaining as described below. 10 µl of NMP was added per well, resulting in a final concentration of 1.82×10^9 (PMMA), 1.76×10^8 (PS), and 1.17×10^{10} (PVC) particles/well.

3.9.4. Immunostaining for widefield imaging

The cells were washed once with 1x Dulbecco's Phosphate buffered saline solution (D-PBS) followed by fixation in 4% formaldehyde at room temperature for 15 min. The cells were washed 3 times with PBS, and autofluorescence was quenched with ammonium chloride (0.1 M, 5 min, room temperature). Triton-X-100 (0.5%) was added for 15 min at room temperature to permeabilize the cells. The plate was washed 3 times, followed by blocking using 5% powdered milk dissolved in TBS-Tween (0.1%) (60 min, room temperature). The plate was incubated at 4°C overnight in mouse anti-NF-κB p65 antibody (Cat. 6956, CST, Danvers, USA) (1:800), followed by washing 3 times in TBS-Tween (0.1%). Secondary antibodies, Alexa Fluor™ 546 – goat anti-mouse IgG (H+L) or Alexa Fluor™ 594 – goat anti-mouse IgG (H+L) in combination with PS samples were used at 4 µg/ml and incubated for 30 min in the dark. Cells were washed in TBS-Tween (0.1%) followed by washing in PBS 3 times before staining the cells using CellMask™ Deep red plasma membrane stain (1:1000 dilution) for 30 min at room temperature, and cells were washed a further 3 times in PBS. Lastly, the nuclei were stained with DAPI (1:1000) at room temperature for 2 min. The final wash was performed in PBS to remove all the excess stain.

3.9.5. Image acquisition and analysis using CellProfiler

Images were captured with widefield imaging using the Cytation™ 5 Cell Imaging Multi-Mode Reader (Biotek Instruments Inc.) at 20x magnification. A 365 LED with DAPI filter cube (Ex 377/50 Em 447/60) was used to detect DAPI staining, a 488 LED with GFP filter cube (Ex 485/20 EM 528/20) to detect PMMA particles, a 523 LED with RFP filter cube (Ex 531/40 Em 593/40)

to detect PS particles, and a 623 nm LED with Cy5 filter cube (Ex 628/40, Em685/40). The acquired images were analyzed using CellProfiler software with the help of the co-supervisor.

3.10. Calculating EC20 for THP-1 cells response to LPS

THP-1 cells were treated with LPS at concentrations ranging from 1 pg/ml to 1000 ng/ml for 18 h. Supernatants were collected and stored at -80°C for analysis of cytokine release by ELISA.

Differentiated macrophages were treated with LPS at the following concentrations (1 pg, 10 pg, 100 pg, 1 ng, 10 ng, 100 ng, 1000 ng/ml) and with IFNγ (20 ng/ml) for 16 h. Cell supernatants were collected and stored at -80°C for analyzing cytokine release by ELISA (refer to section 3.12).

We calculated the EC20 value for the induction of TNFα in response to LPS using non-linear regression (curve fit) with log(agonist) vs. response – Find ECanything model in GraphPad Prism.

3.11. Gene expression analysis by quantitative (q) PCR

3.11.1. RNA extraction

Complete/Total RNA was isolated from the cells using Qiagen's RNeasy® Mini kit (250) or Omega BIO-TEK's E.Z.N.A.® Total RNA kit I by following the manufacturer's instructions. The isolated RNA was stored at -80°C. The NanodropTM One/OneC Microvolume UV-Vis Spectrophotometer (ND-ONE-W) from Thermo Fisher Scientific was used for the quantity and purity of RNA. Measurement of RNA concentration with A260/A230 absorbance between 1.8 - 2.1 and A260/280 absorbance between 2.0-2.2 was acceptable.

3.11.2. Reverse transcription and qPCR

Reverse transcription was performed with 0.5-1 µg of RNA per sample using the QuantiTect® Reverse Transcription Kit from Qiagen, as per the manufacturer's protocol. The real-time PCR analysis was performed as instructed by the manufacturer using Roche's LightCycler® 480 SYBR® Green I Master MIX and LightCycler® 96 Instrument. The program set for the PCR and the list of primers used is shown in Appendix D.

3.11.3. qPCR data analysis

LinRegPCR version:2019.1 was used to analyze amplification curves generated by the LightCycler® 96 instrument to measure PCR efficiency per amplicon and calculate Ct. values per

sample [79]. The PCR data were statistically analyzed (one-way ANOVA) using qbase+, version 3.2 (Biogazelle, Zwijnaarde, Belgium – www.qbaseplus.com) [80].

Selection of reference genes

For calculating relative quantity, normalization of the data is required for accuracy. The following reference genes were chosen for normalization: *ACTB, GAPDH,* and *RPS18* [81-83].

3.12. Cytokine release by Enzyme-Linked Immunosorbent Assay (ELISA)

The concentration of cytokines TNFα, IL-6, and IL-10 in the cell supernatants were determined by ELISA using the DuoSet ELISA kits (R&D Systems, Minneapolis, MN, USA). The protocol was followed according to the manufacturer's instructions.

MyAssays, an online analysis tool, was used to analyze the ELISA results. A four-parameter logistic curve fit was used to conduct the analysis. The average of all replicates determined the plotted values for each treatment ± SD (www.myassays.com).

3.13 Statistical analyses

In this study, a biological replicate is defined as an independent experiment in which the cells are seeded from different culture flasks. A technical replicate consists of wells plated using cells from the same flask.

GraphPad Prism version 9.2.0 (GraphPad Software, La Jolla California USA, www.graphpad.com) was used for statistical analysis. Using an ordinary one-way ANOVA with Dunnett's multiple comparisons test. P-values < 0.05 were considered statistically significant.

4 Results

4.1. Particle characterization

Nanoparticle tracking analysis (NTA) was performed to measure the size distribution and concentration of the polydisperse PMMA, PS, and PVC particles (refer to 3.3).

The particle size distributions of the stock suspensions obtained from the NTA measurements were fit to a Lognormal distribution (Figure 4.1). The size distribution of the PMMA, PS, and PVC suspensions ranged broadly from 70-600 nm, and the mean particle size values were 186 nm (PMMA), 174 nm (PS), and 216 nm (PVC), with 50% of the particles being ≤150 nm (PMMA), ≤147 nm (PS), and ≤199 nm (PVC). The concentration of the stock suspensions was found to be 2.73×10^{11}/ml (PMMA), 2.65×10^{10}/ml (PS), and 1.75×10^{12}/ml (PVC).

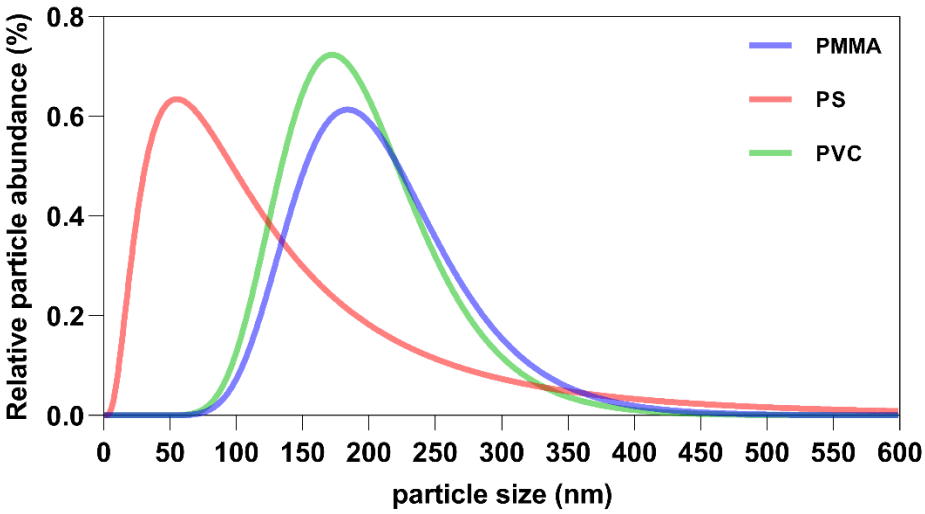

Figure 4.1. Size distribution of the NMP suspensions determined by nanoparticle tracking analysis. The graph represents the relative particle abundance (%) of the PMMA, PS, and PVC in particle stock suspensions. Particle abundance was fit to a lognormal function showing the distribution in %.

When exposing primarily adherent cells (macrophages) in culture to the particles, we considered that the varying likelihood of particles of different sizes to 'settle' to the bottom of the well might affect the relative exposure of the cells. We, therefore, attempted to measure the time taken for the different plastic particles of different sizes to settle to the bottom of a cell culture well.

To do this, we used time-lapse confocal microscopy. The wells of a chamber slide were filled with 300 µl of media, and 30 µl of plastic particles were added. The focus was maintained on the cover glass at the bottom of the well, and we imaged the well for 10-16 h. Individual experiments were

carried out for PMMA, PS, and PVC particles. The images from CLSM were analyzed using CellProfiler software (refer to 3.4).

The PMMA particles settle fast, with a high number of particles settled by 10 h (Figure 4.2 (a)). For PS, the particles settle slower by 15 h (Figure 4.2 (b)), whereas for PVC, the settling time of the particles looked quite similar by 6 and 10 h (Figure 4.2 (c)). Overall, smaller particles tend to settle slower when the particle size takes more than 5 hours to reach the bottom of the well.

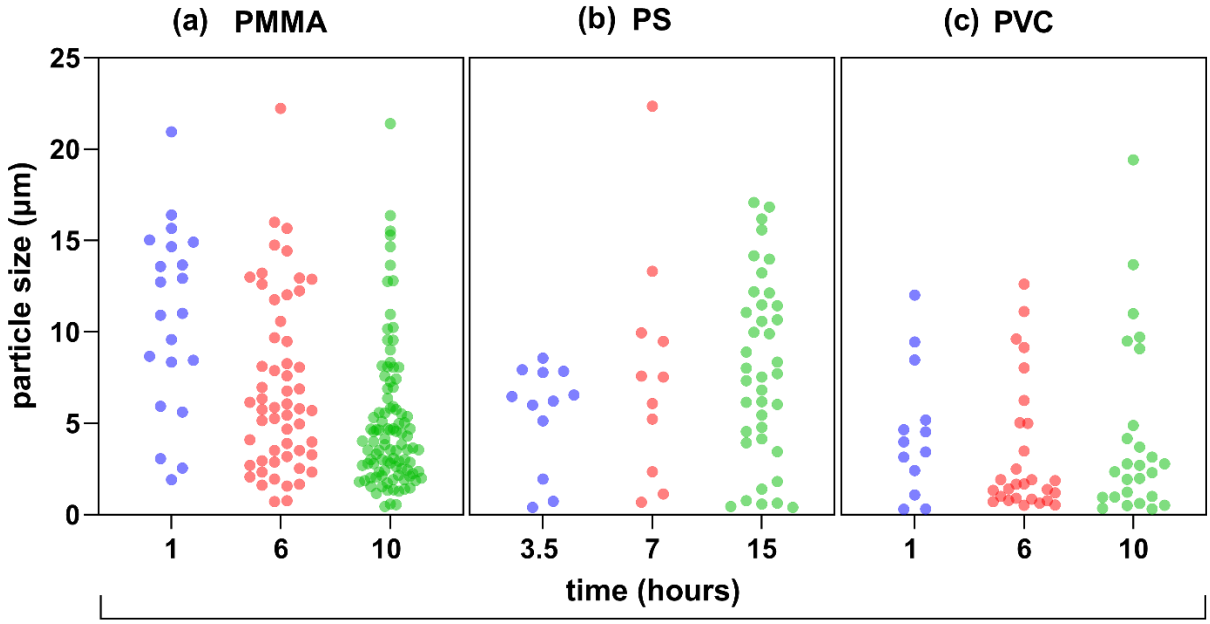

Figure 4.2. Time and size-dependence of particle settling determined by time-lapse confocal microscopy for (a) PMMA, (b) PS, and (c) PVC. Image analysis to determine particle number and size was carried out using CellProfiler software.

The size distribution of the settled particles was calculated and fit to a Lognormal distribution (Figure 4.3). Compared to the NTA analysis of stock solutions, settled particles were considerably larger (1-20 µm). The limits of light microscopy mean that particle ≤ 200 nm cannot be resolved. However, it is still apparent that the settled particles are considerably larger than the distribution of the particles in the stock suspensions, which may play a role in the effect of the NMPs on macrophages using *in vitro* assays.

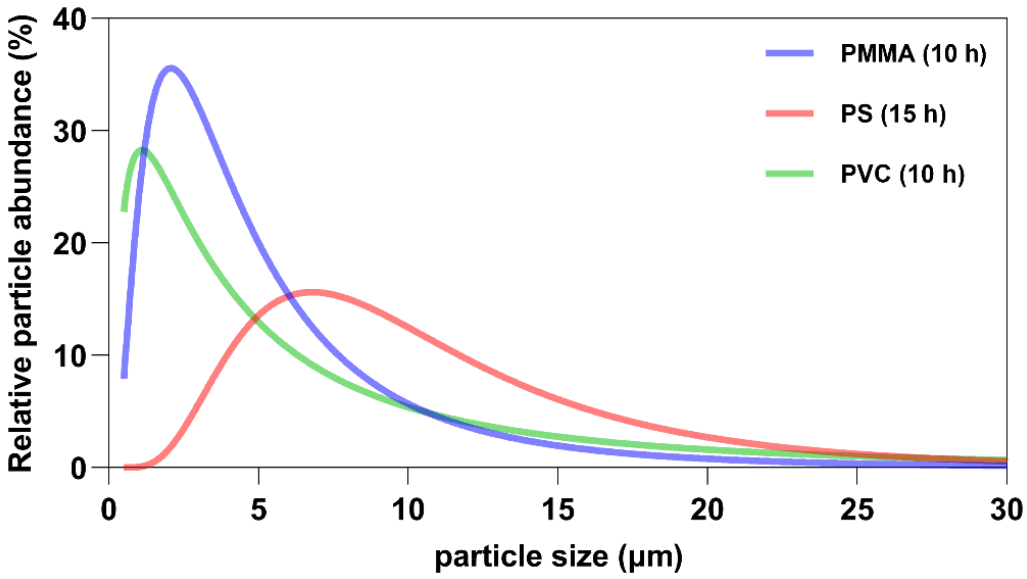

Figure 4.3. Particle size distribution of the settled NMP's determined using confocal microscopy. The graph represents the relative particle abundance (%) of the PMMA at 10 h, PS at 15 h, and PVC at 10 h after addition to the media. The relative particle abundance was fit to a lognormal fit, showing the distribution in %.

4.2. Cytotoxicity of NMP's in THP-1 monocytes and THP-1 derived macrophages

To determine whether the NMP's are cytotoxic to THP-1 cells, viability assays were performed as described above. Serial dilutions of the NMP's were prepared, and THP-1 monocytes and THP-1 derived macrophages were exposed for either 24- or 72 h. The cell viability was measured by resazurin assay. The final particle concentrations that the cells were exposed to are shown in Table 3.1.

Treatment with PS at the highest concentration (**1**) decreased monocyte viability by 10% after 24 h. Neither PVC nor PMMA affected monocyte viability after 24 h (Figure 4.4 (a)). By 72 h, cells with PS treatment decreased cell viability by 15% in the highest concentrations (**1** and **2**). PMMA reduced the viability by 10% at the high concentration (**1**) (Figure 4.4 (b)). PVC did not affect viability up to 72 h.

In THP-1 derived macrophages after exposed for 24 h, PVC treatment reduced cell viability by 10% at the highest concentration (**1**), whereas PMMA and PS had no significant effect (Figure 4.5 (a)). By 72 h, PVC treatment significantly reduced cell viability at concentrations (**1** to **7**) with a maximum reduction of 30% at the highest concentration. PMMA treated cells, and PS treated cells viability were decreased by 15% in the higher concentrations (**1, 2,** and **3**) (Figure 4.5 (b)).

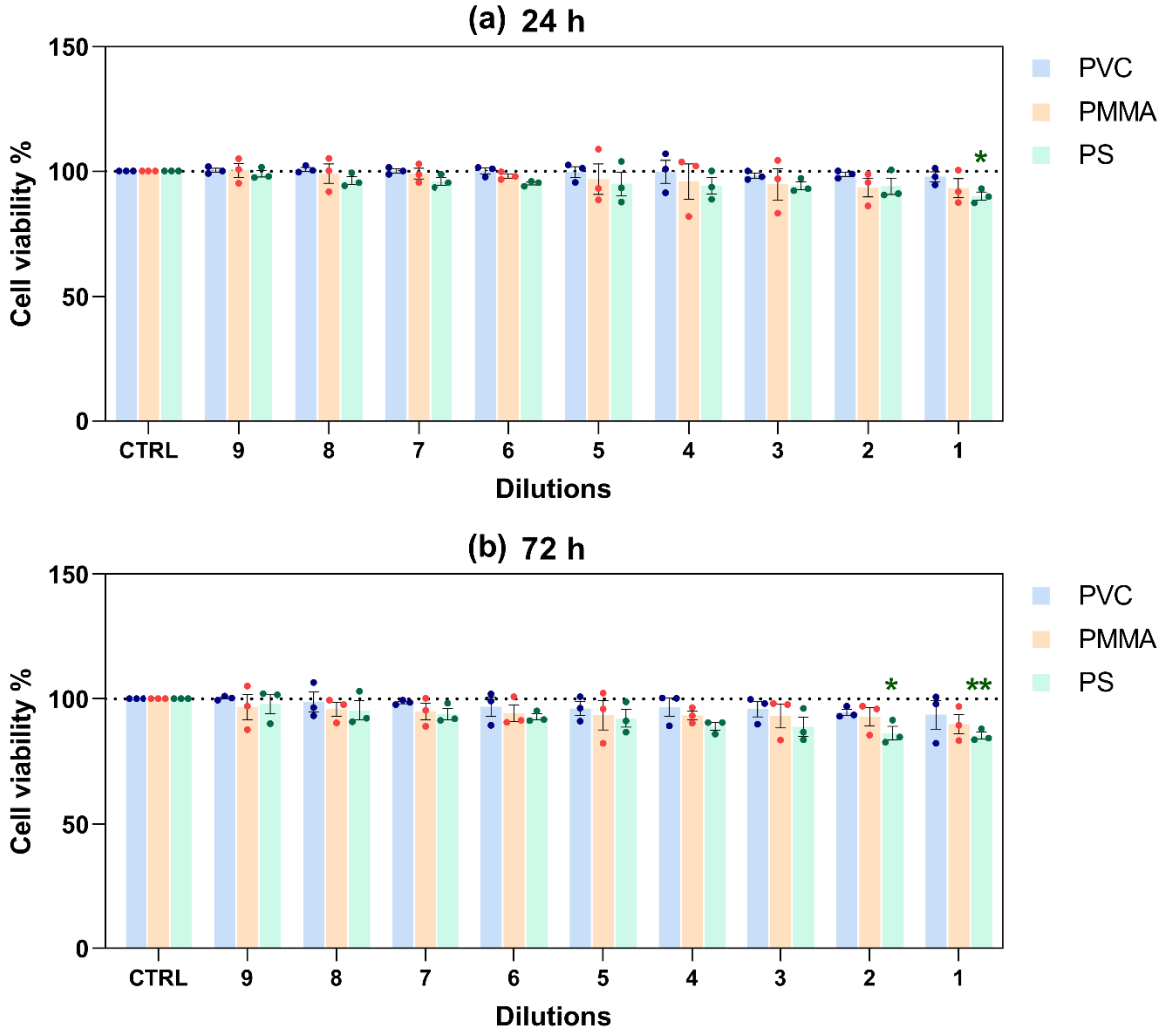

Figure 4.4. Cytotoxic effects of NMP's in THP-1 monocytes. THP-1 cells were exposed to NMP's for indicated time points. The cell viability was measured by resazurin assay. The bar graph shows the viability of cells after NMP treatment for **(a)** 24 h and (**b)** 72 h. The control (no plastic treatment) was set to 100% viability. Data shown in % viability are the mean ± SEM of 6 technical replicates from 3 independent experiments (n=3). *= $p < 0.05$, **= $p < 0.01$ compared to the control (CTRL)

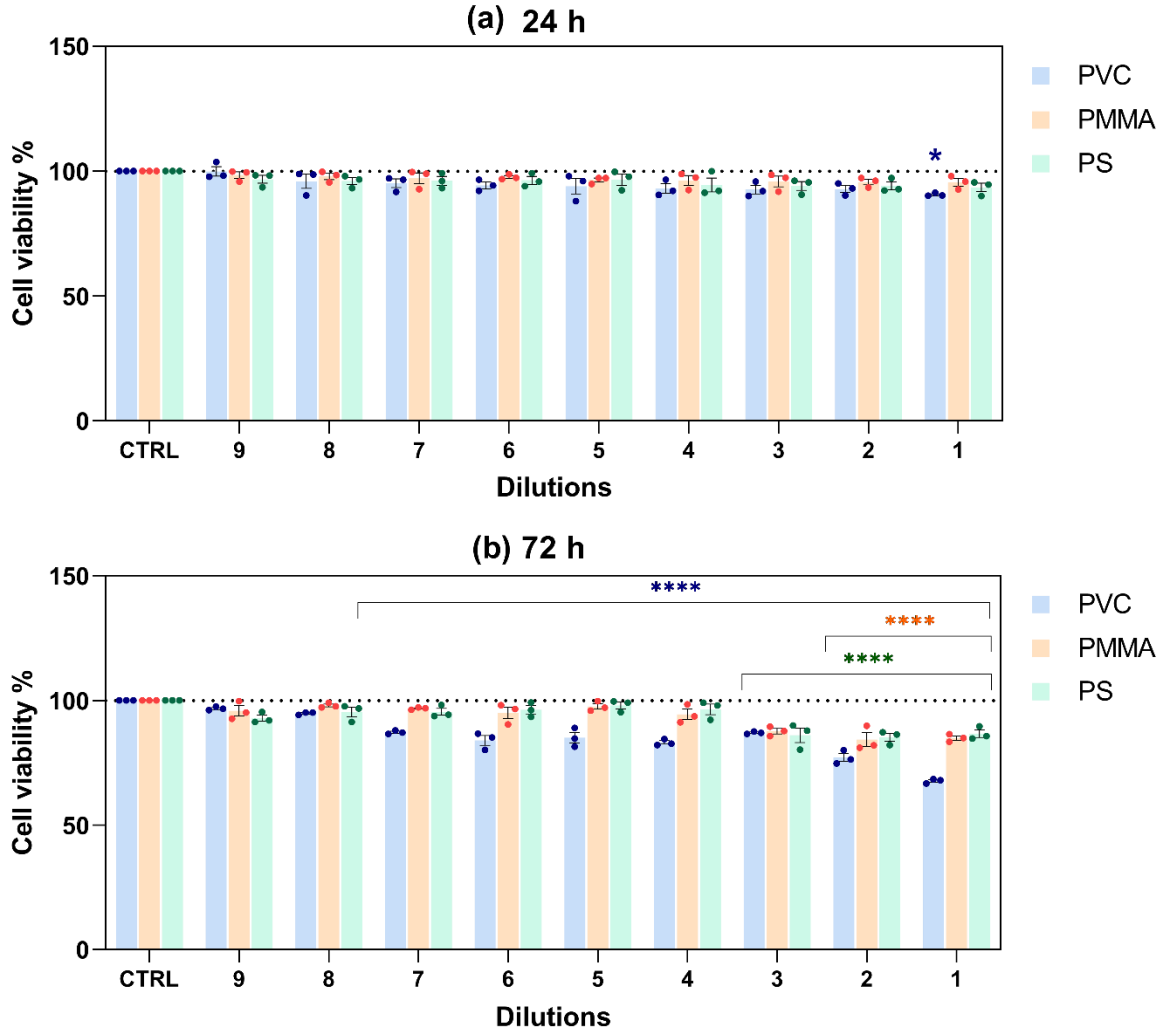

Figure 4.5. Cytotoxic effects of NMP's in THP-1 derived macrophages. Macrophages were exposed to NMP's for indicated time points and measured the cell viability by resazurin assay. The bar graph shows the viability of cells after NMP treatment for **(a)** 24 h and (**b)** 72 h. The control (no plastic treatment) was set to 100% viability. Data shown in % viability are the mean ± SEM of 6 technical replicates from 3 independent experiments (n=3). *= $p < 0.05$, ****= $p < 0.0001$ compared to the control (CTRL)

From the results, we can conclude that PS particles were slightly toxic at the highest concentration in THP-1 monocytes after both time points. By 72 h, PVC, PMMA, and PS showed significant toxicity over a range of concentrations in THP-1 derived macrophages.

4.3. NMP's were internalized by THP-1 derived macrophages

Macrophages are phagocytic cells, which play a significant role in the innate immune system. They can engulf anything foreign to the body, including dead cells, dust, pollen, and plastic particles [84]. Being professional phagocytes, they are capable of efficient particle uptake through

phagocytosis [85]. The phagocytic behavior of macrophages is one of the fundamental properties that define their role in the human defense response and the production of various pathologies [86].

We wanted to investigate whether the THP-1 derived macrophages internalize NMP's. To do this, we exposed the macrophages to the plastic particles for either 30 min or 16 h. The cell membrane was stained with Cell Mask deep red stain, and live imaging with confocal laser scanning microscopy (CLSM) was performed. Both the PMMA and PS particles were fluorescent, and non-fluorescent PVC particles were stained with NileRed before exposure to allow their visualization. In order to determine whether plastic particles were inside the cell, we performed z-stacking and 3D reconstruction.

The left side images show a single slice obtained from the z-stack imaging of PMMA (Figure 4.6), PS (Figure 4.7), and Nile Red stained PVC (Figure 4.8) exposed macrophages for either 30 min or 16 h. The right-side images show the orthogonal view of z-stacks, which allows the visualization of the 3D view of the z-stacking series in a single x-y plane and were used to show whether the plastic particles were attached to or within the cell.

Following exposure of the different NMP's for 30 min, most of the particles were seen to be attached to the cell membrane but not internalized. After 16 h of exposure, many plastic particles were fully internalized by the macrophages.

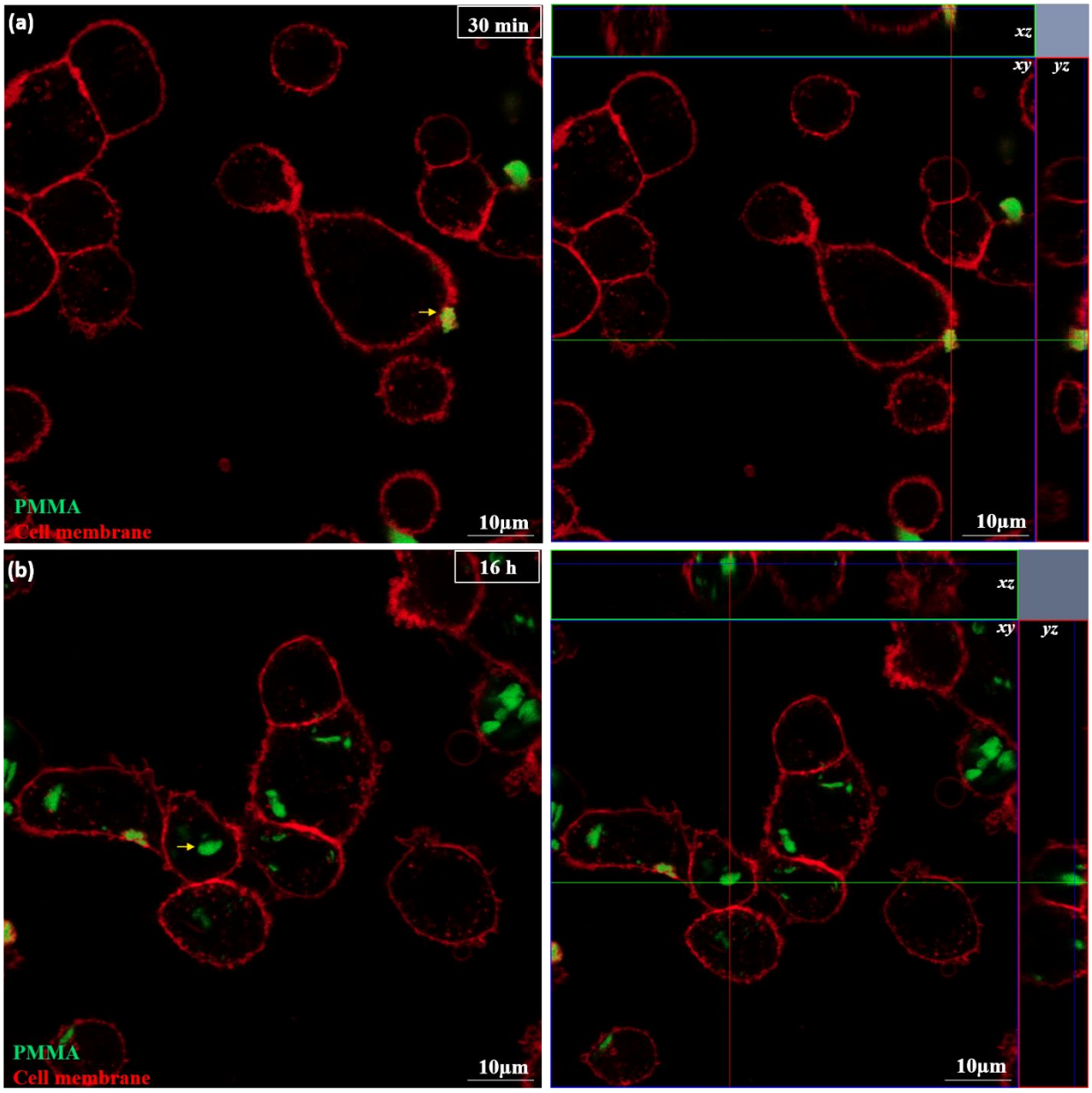

Figure 4.6. Representative images showing the internalization of PMMA in THP-1 derived macrophages. Macrophages were exposed to PMMA for **(a)** 30 min or **(b)** 16 h. The cell membrane was stained, and the cells were imaged live using confocal microscopy with a 63x/1.4 oil immersion. 27-37 z-stacks were taken for 3D projection. The left image shows a single slice from the z-stack, and the right image shows the orthogonal view (x-y projection along with respective side views (x-z and y-z projections)).

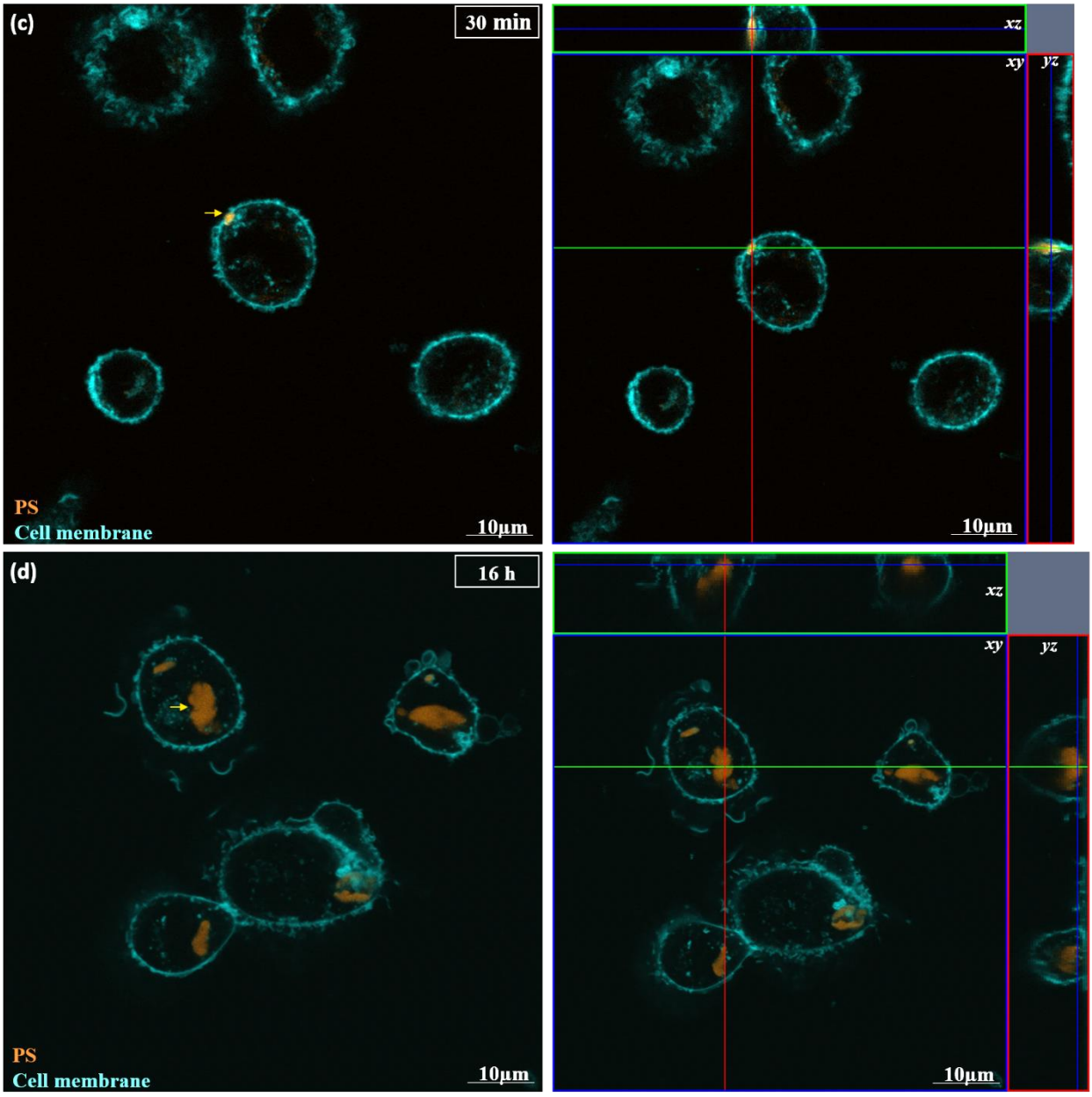

Figure 4.7. Representative images showing the internalization of PS in THP-1 derived macrophages. Macrophages were exposed to PS for **(a)** 30 min or **(b)**16 h. The cell membrane was stained, and the cells were imaged live using confocal microscopy with a 63x/1.4 oil immersion. 30 z-stacks were taken for 3D projection. The left image shows a single slice from the z-stack, and the right image shows the orthogonal view (x-y projection along with respective side views (x-z and y-z projections)).

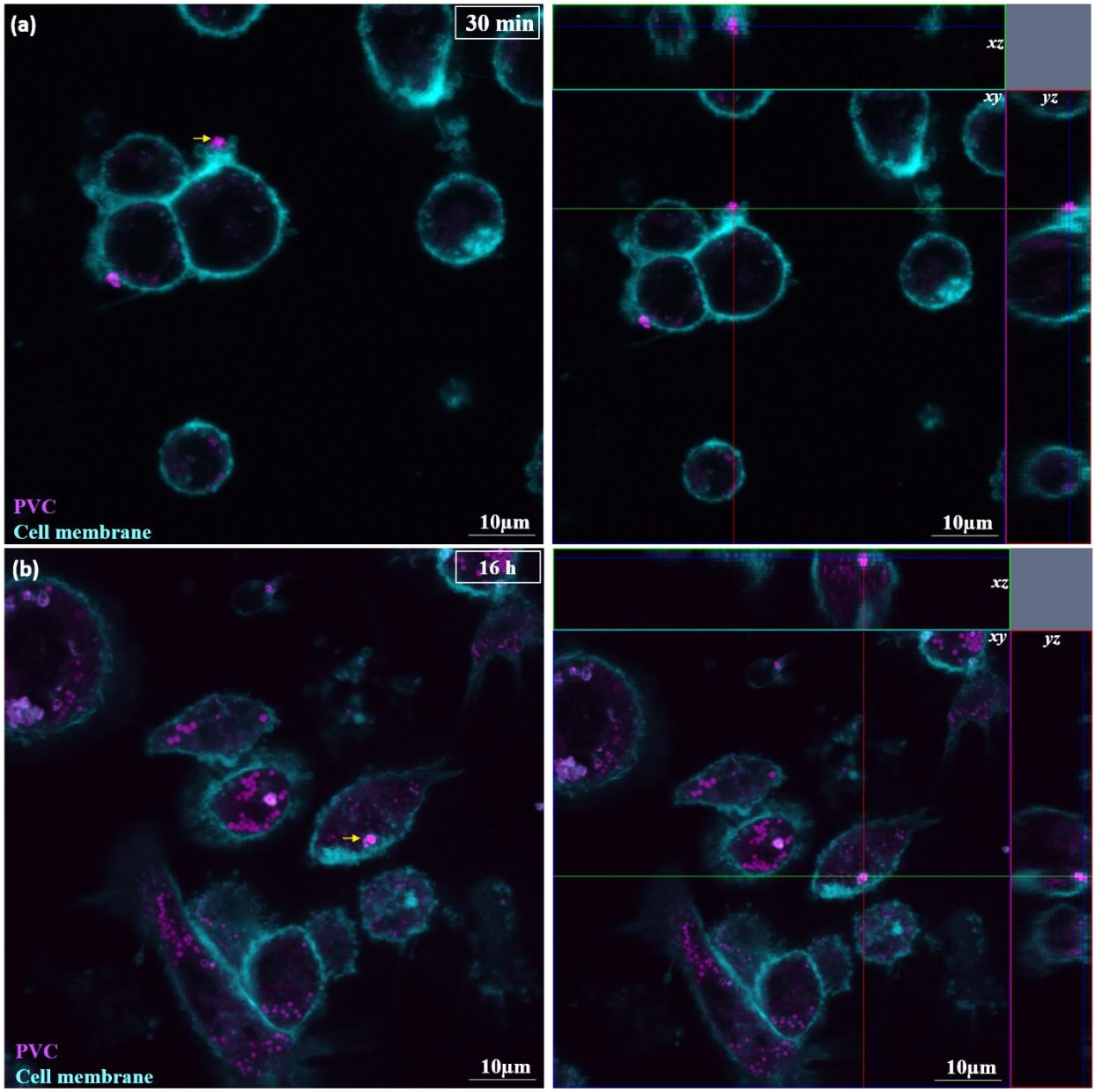

Figure 4.8. Representative images showing the internalization of PVC in THP-1 derived macrophages. Macrophages were exposed to Nile Red stained PVC particles for **(a)** 30 min or **(b)** 16 h. The cell membrane was stained, and the cells were imaged live using confocal microscopy with a 63x/1.4 oil immersion. 14-19 z-stacks were taken for 3D projection. The left image shows a single slice from the z-stack, and the right image shows the orthogonal view (x-y projection along with respective side views (x-z and y-z projections)).

Nile Red (a lipid staining dye) was used to stain the PVC particles before exposing them to the macrophages to enable us to visualize their internalization. However, the Nile Red dye binds not only to the plastic particles but to lipids as well. Therefore, it was necessary to perform additional control experiments for PVC to show the difference between lipid droplets and Nile Red-stained PVC particles by staining the macrophages with Nile Red alone. Control staining (without the

dyed plastic particles) showed a uniform circular staining pattern with lower intensity. The plastic particles, on the other hand, were typically less uniform (non-circular) and higher intensity, as shown in Figures 4.9 (a) and (b). Uniform lipid droplets are indicated with a yellow box, while the less-regular and brighter Nile Red stained-PVC particles are indicated with arrows. From this, we could distinguish the lipid droplets from the PVC particles.

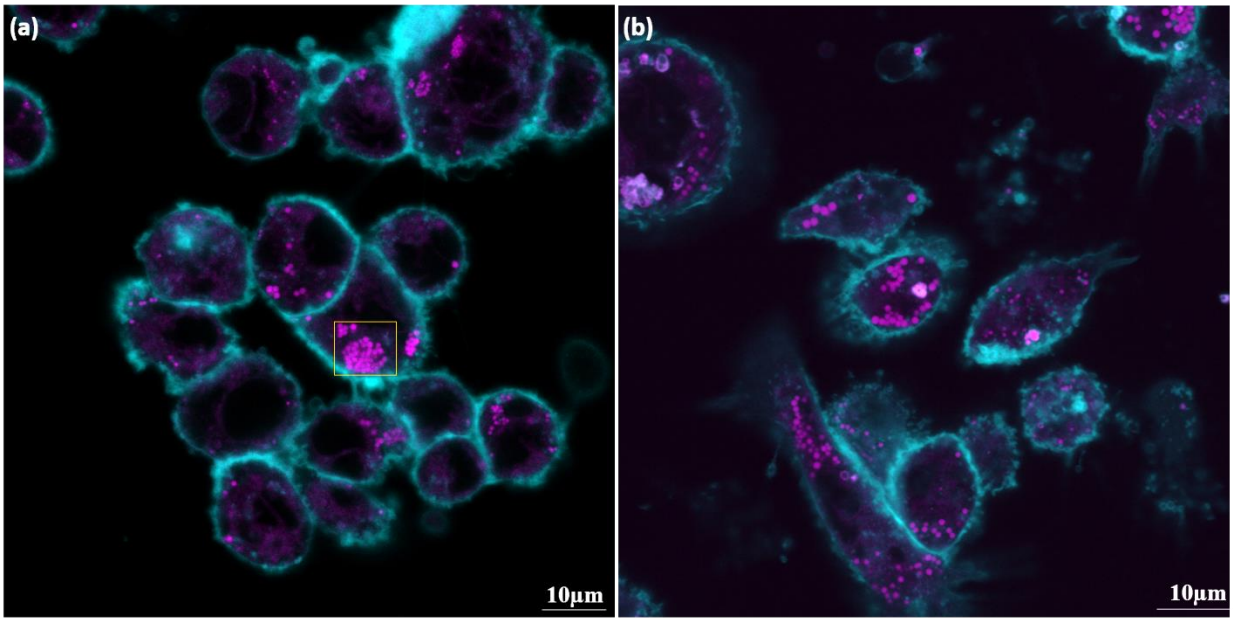

Figure 4.9. Representative images showing Nile Red staining in untreated and PVC treated macrophages. THP-1 derived macrophages were treated with Nile Red and Nile Red-stained PVC for 16 h. **(a)** Control staining with Nile Red alone shows lipid droplets (marked with a yellow box) and **(b)** shows the identification of Nile Red stained PVC particles (indicated with yellow arrows) along with the lipid droplets (yellow box).

We carried out a similar experiment in cells that were fixed after 30 min, 2 h, or 16 h and stained with the cell membrane dye post-fixation. The cell membrane staining was not as well-defined as when the staining was performed in live cells, presenting a limitation to accurate determination of particle internalization. We do, however, see similar results, and these images are presented in Appendix E.

Thus, we determined that THP-1 derived macrophages internalized all three NMP types and that this occurred within 16 h of exposure.

4.4. Investigating whether exposure to NMP's can cause inflammatory responses and polarization of THP-1 derived macrophages

Given that the THP-1 derived macrophages internalized all three types of NMP after exposure for 16 h but caused little or no cytotoxicity by 24 h, we were interested in finding out whether particle internalization resulted in an inflammatory response that might be observed from exposure to pathogens. To investigate this, we measured **(1)** the activity of the transcription factor NF-κB, **(2)** the expression of genes associated with polarization to a pro-inflammatory phenotype (M1), and **(3)** the release of pro-inflammatory cytokines IL-6 and TNFα.

4.4.1. Optimization of NF-κB translocation assay

When macrophages are exposed to bacterial products such as LPS, the activation of the NF-κB transcription factor occurs, regulating the gene expression system that underlies macrophage-dependent immune response [87]. Signals induced by the external stimuli result in the activation of NF-κB regulated by its cellular localization, translocated from the cytoplasm of the cell into the nucleus. Thus, the activated NF-κB induces and regulates the expression of various pro-inflammatory genes [88]. Immunofluorescence microscopy can be used to visualize and quantify the translocation of NF-κB [78].

First, we wanted to determine at which time-point the NF-κB activity was maximum when THP-1 derived macrophages are stimulated with LPS. Also, we wanted to assess if resting the differentiated macrophages for 2- and 5 d post-PMA stimulation influences the translocation of NF-κB/enhance the activity of NF-κB upon LPS stimulation.

The ratio of nuclear: cytoplasmic NF-κB showed a gradual increase from 15 min with maximum nuclear translocation observed at 120 min after both 2- and 5-days of resting (Figure 4.10).

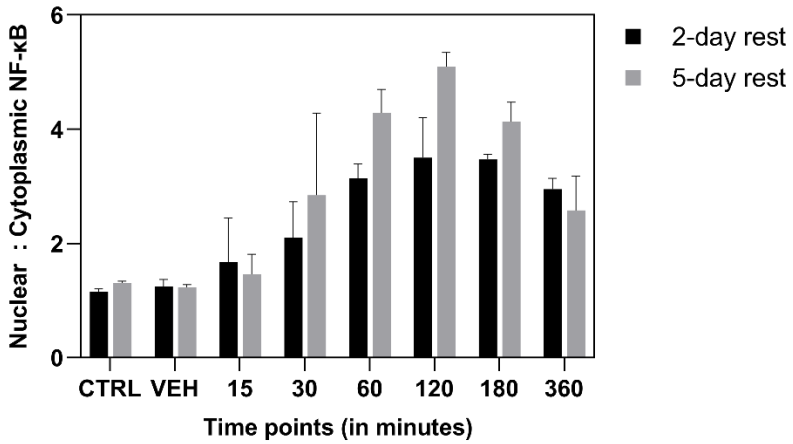

Figure 4.10. Time-dependent translocation of NF-κB in LPS stimulated macrophages. After 2- and 5-day resting, THP-1 derived macrophages were treated for the indicated times with LPS (100 ng/ml). Data are the mean ± standard deviation of 6 technical replicates from a single experiment. CTRL = macrophages, VEH = DMSO + PBS

Figure 4.11 (a) and (b) show the difference between unstimulated cells containing the NF-κB in the cytoplasm. At 120 min, after the LPS stimulation, the bright nucleus indicates the translocation of NF-κB from the cytoplasm into the nucleus.

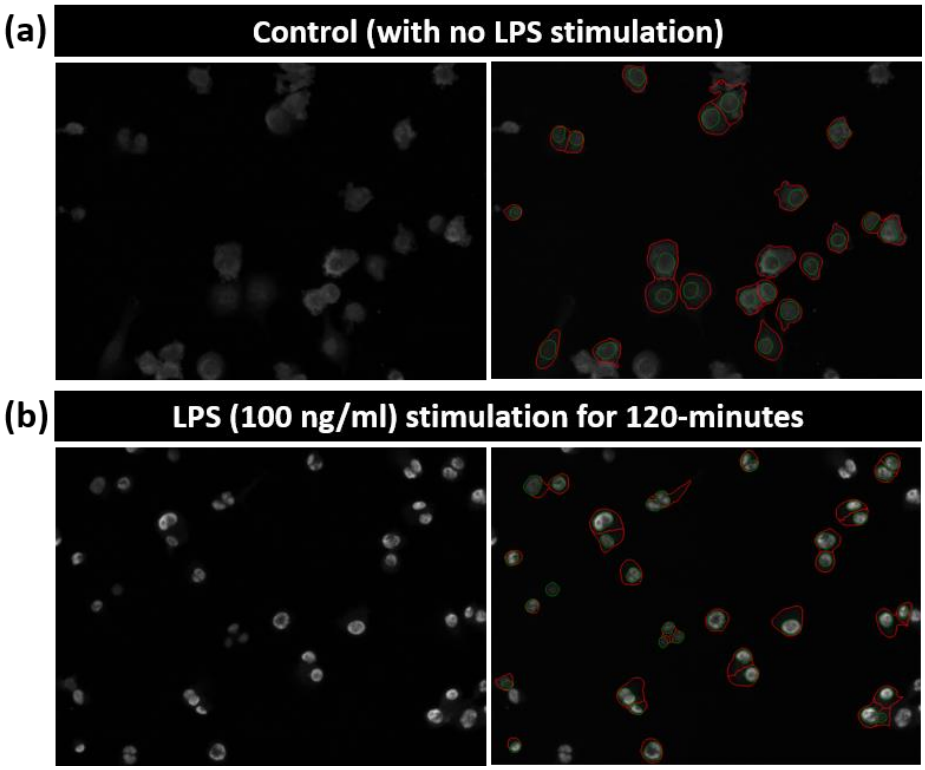

Figure 4.11. Representative images of NF-κB nuclear translocation in THP-1 derived macrophages. Images show immunofluorescence using NF-κB antibody for **(a)** unstimulated macrophages and (**b)** following stimulation with 100 ng/ml LPS for 120 min. Images in the right panel show the segmentation of nuclei (green) and cells (red) carried out in CellProfiler and used to calculate the nuclear:cytoplasmic ratios.

4.4.2. Effect of NMP's on NF-κB translocation

To test whether exposure of THP- 1 derived macrophages to NMP's can induce NF-κB activation, we treated the cells with the highest concentration of NMP's (PVC, PMMA, PS) for the time-points mentioned. 100 ng/ml of LPS stimulation for 2 h was used as a positive control. Similar to the control experiment above, Fluorescence images of the fixed and immunofluorescence-stained cells were captured and analyzed using the CellProfiler software. 2-3 independent experiments were carried out using 3 technical replicates per condition. PBS was used as vehicle control for PVC, PMMA, and PBS + 1:10,000 Tween 20 for PS.

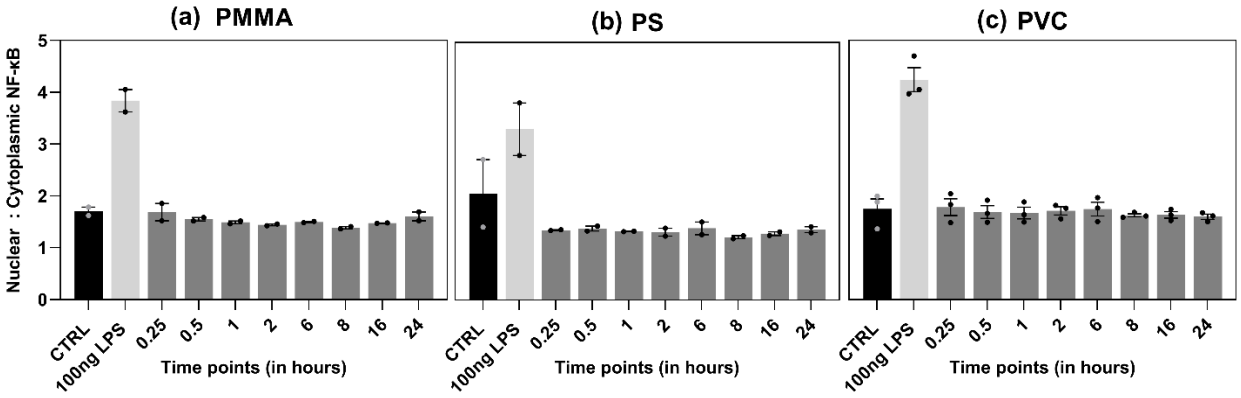

Figure 4.12. Analysis of NF-κB translocation in response to NMP exposure. THP-1 derived macrophages were treated with different NMP for the time periods indicated. 100 ng/ml LPS stimulation for 2 h was used as a positive control. The bar graph represents the ratio of nuclear:cytoplasmic NF-κB for **(a)** PMMA **(b)** PS **(c)** PMMA. 6 technical replicates were carried out per sample, and the data points shown are the mean ± standard deviation from 2 biological replicates (for PMMA and PS) and 3 biological replicates (for PVC).

We did not observe any translocation of NF-κB in response to treatment with the NMP's, whereas LPS treatment caused an approximately 2-fold increase in the nuclear:cytoplasmic ratio. From the results, we can conclude that the NMP's were unlikely to activate NF-κB using the conditions described (Figure 4.12).

4.4.3. Optimization of the protocol to polarize the THP-1 derived macrophages

Macrophages polarize in response to microenvironmental signals. By secreting cytokines and producing reactive oxygen species (ROS), they may function in a pro- or anti-inflammatory manner, often termed M1 or M2 polarization, respectively. Macrophages can be polarized to an M1 (pro-inflammatory) phenotype by stimulation with IFNγ combined with LPS for 24 h [62]. Most studies use IFNγ at a 20 ng/ml concentration, while LPS concentrations used can range from

10 pg to 1 µg/ml [89]. Allowing the differentiated cells to rest for up to 5 d before stimulation has been reported to affect the ability of macrophages to polarize [50].

Here we investigated whether allowing the differentiated macrophages to rest after PMA removal for between 1 and 5 d affected the ability of the cells to respond to M1 polarization stimuli. Macrophages were stimulated using IFNγ (20 ng/ml) with either a low concentration (10 pg/ml) or a high concentration (100 ng/ml) of LPS.

M1 polarization was assessed by measuring the gene expression levels of *CCL2, TNFα,* and *IL-12* as three genes commonly up-regulated in M1 polarized macrophages, as described [64].

CCL2 and *TNFα* were up-regulated in response to IFNγ + either 100 ng/ml LPS or 10 pg/ml LPS with a larger response in the macrophages treated with 100 ng/ml LPS. Resting the differentiated cells for different lengths of time did not have a clear or consistent impact on the induction of these M1 polarization markers, with the possible exception of higher induction of *TNFα* expression with an increasing rest period, only when using the lower dose of LPS (Figure 4.13 (a) and (b)). *IL-12* was up-regulated to a lesser extent than *CCL2* and *TNFα*. The response was only significant using the lower dose of LPS and following 2 or more days of resting before polarization (Figure 4.13 (c)).

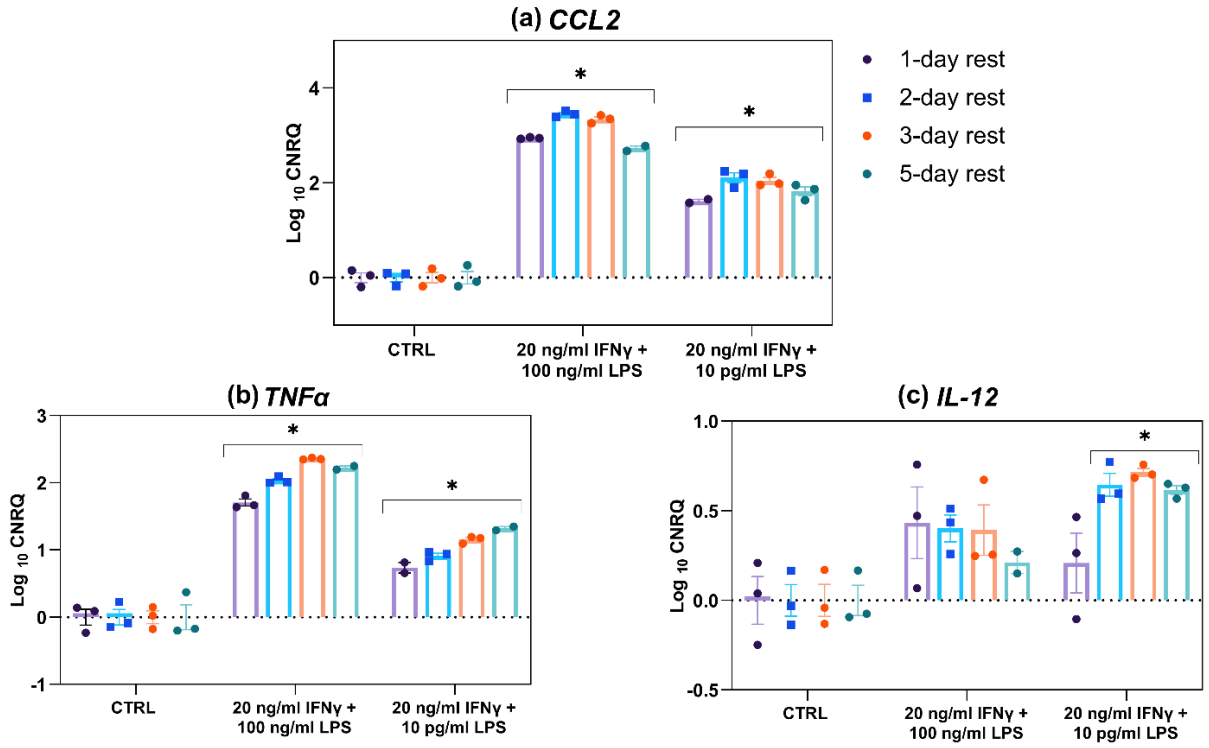

Figure 4.13. Relative expression of M1 macrophage marker genes. THP-1 derived macrophages were incubated with either vehicle (CTRL) or IFNγ (20 ng/ml) and LPS (100 ng/ml or 10 pg/ml) for 16 h after the stated number of resting days. The expression of **(a)** *CCL2* **(b)** *TNFα* and **(c)** *IL-12* was measured by qPCR. Data were normalized to three reference genes and expressed relative to the respective unstimulated controls at each time-point (CNRQ) ± SEM. The experiment was performed three times (n=3). Statistical analysis was carried out by one-way ANOVA in qbase software. * = $p < 0.05$ compared to control (CTRL)

We concluded that resting the differentiated macrophages for up to 5 days did not significantly impact the effect of M1 polarization stimuli. In subsequent experiments, we rested the macrophages for two days before exposure to the NMP's, and 20 ng/ml IFNγ with 100 ng/ml LPS (for 16 h) was used as a positive control for M1 polarization.

4.4.4. Effect of NMP's on macrophage polarization

To determine whether NMP exposure causes M1 polarization of THP-1 derived macrophages, the cells were exposed to PMMA, PS, or PVC at the highest particle concentration for 16-, 48-, or 72 h. The expression of a panel of genes associated with M1-polarization (*CCL2*, *TNFα*, *COX2*, *IL-6*, *IL-12*, *IL-1β,* and *SOCS3*) was measured by qPCR.

These genes were selected based on studying the literature, as reviewed [64]. IFNγ + LPS (M1 polarization positive control) induced the expression of *CCL2*, *TNFα, IL-6*, *IL-1β, SOCS3, COX2,* and *IL-12*. While exposure to NMP had no effect on the expression of any of the genes tested

(Figure 4.14). The control here denotes the negative control for PMMA and PVC (with PBS); the negative control for PS (with PBS + 1:10000 Tween 20) could not be used for the analysis, as the RNA quantity was too low due to technical problems.

The same gene expression analysis was performed for macrophages exposed to the NMP's for 48 and 72 h, but again, no induction of M1 polarization was observed (results Appendix F).

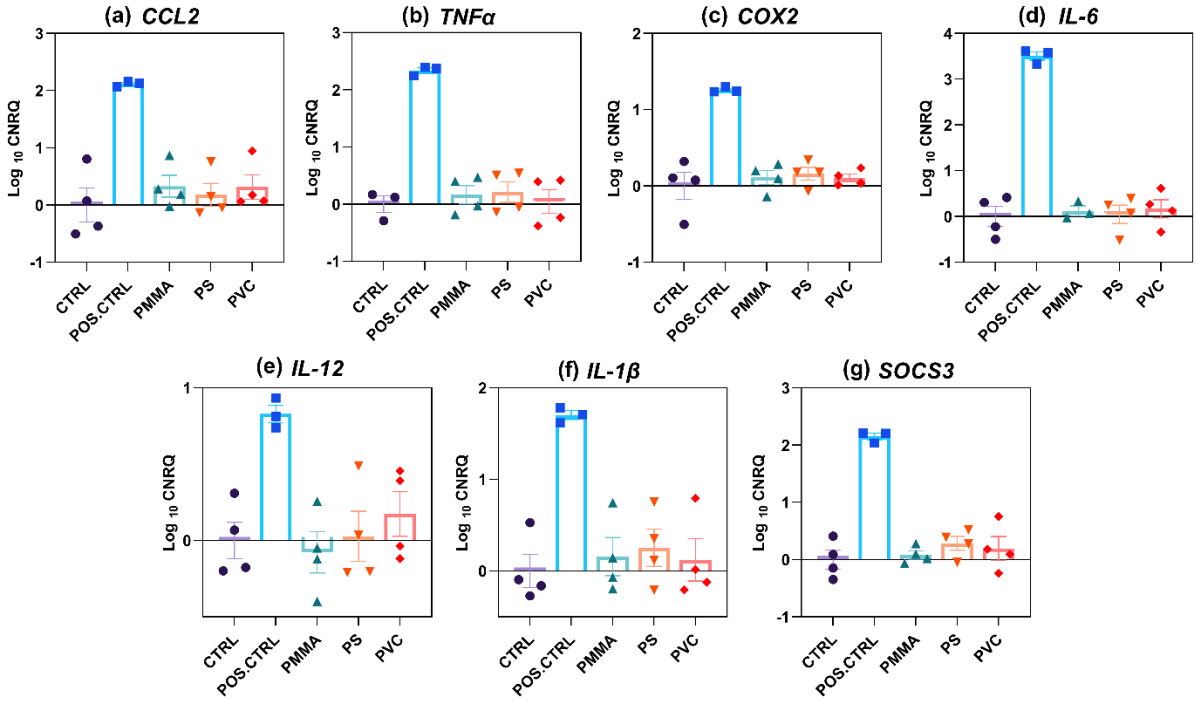

Figure 4.14. Relative expression of M1 macrophage marker genes in macrophages exposed to NMP's. THP-1 derived macrophages were exposed to vehicle (CTRL), 20 ng/ml IFNγ + 100 ng/ml LPS (POS.CTRL), or to PMMA, PS, or PVC at the highest particle concentrations for 16 h. Graphs show the relative gene expression for **(a)** *CCL2* **(b)** *TNFα* **(c)** *COX2* **(d)** *IL-6* **(e)** *IL-12* **(f)** *IL-1β* and **(g)** *SOCS3* measured using qPCR. Data were normalized to three reference genes, and the mean expression relative to the vehicle-treated control (CTRL) (CNRQ) ± SEM is shown. Data for the NMP exposures represent the results from four independent experiments (n=4), while the positive control data is obtained from 3 technical replicates. Statistical analysis was carried out with one-way ANOVA in qbase+.

4.4.5. Effect of NMP's on cytokine secretion

Cell supernatants from the above experiments were collected and analyzed for pro-inflammatory cytokine production (TNFα and IL-6) by ELISA. Supernatants from the positive control (M1) macrophages had an average of 4587 pg/ml TNFα (Figure 4.15 (a)) and 1276 pg/ml IL-6 (Figure 4.15 (b)). The levels of both TNF-α and IL-6 were below the limit of detection for both in the vehicle controls.

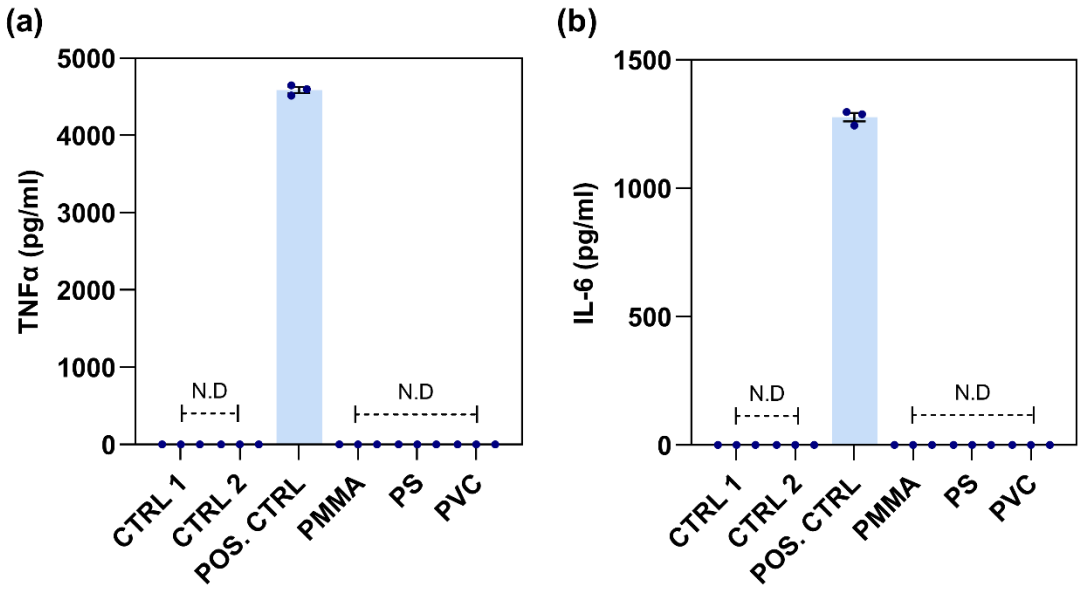

Figure 4.15. Cytokine release in macrophages exposed to NMP's. THP-1 derived macrophages were treated with different NMP's for 16 h. Cytokine released by macrophages was measured by ELISA, **(a)** TNFα **(b)** IL-6. Results are shown as mean ± SEM across three biological replicates (n=3). No statistical analysis was done as only the positive control was detected. CTRL 1 = PBS, CTRL 2 = PBS + 1:10,000 Tween20, POS.CTRL = 20 ng/ml IFNγ + 100 ng/ml LPS]

In conclusion, we showed that exposure of THP-1-derived macrophages to the highest concentration of any of the three NMP's did not induce the activation of NF-κB, M1 polarization, or the secretion of pro-inflammatory cytokines, and was therefore unlikely to have caused a pro-inflammatory response in this cell type.

4.4.6. Effect of NMP's on M1 polarized macrophages

The results above showed that exposure to NMP's did not trigger an inflammatory response in the control macrophages. We, therefore, next investigated whether NMP exposure could affect the pro-inflammatory response to LPS. To do this, we first determined the EC20 of LPS stimulated TNFα release to ensure that the system was not saturated. To find the EC20, we performed an LPS dose-response in combination with 20 ng/ml IFNγ. LPS concentrations varied from 1 pg/ml to 1 µg/ml, and the treatment was for 16 h. The cell supernatants were analyzed for TNFα by ELISA.

We observed detectable and dose-dependent release of TNFα in response to LPS in between 1 pg/ml and 1 µg/ml. EC20 was calculated as 20 pg/ml (refer to section 3.10, Figure 4.16) shows the LPS dose-response curve in TNFα, where the different LPS concentrations are shown in log-values.

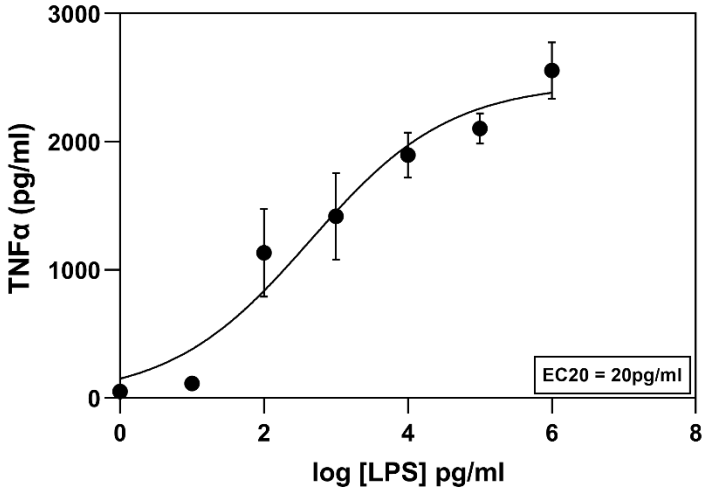

Figure 4.16. Dose-dependent release of TNFα in response to LPS. Macrophages were treated with 20 ng/ml IFNγ + LPS at the concentrations indicated for 16 h. Cell supernatants were harvested and analyzed for TNFα cytokine release by ELISA. Non-linear regression was used to fit the data to a curved and determine the EC20. Data are the mean ± SEM of three technical replicates.

THP-1 derived macrophages were thus treated with 20 ng/ml IFNγ + 20 pg/ml LPS in the presence or absence of the NMP's for 16 h. Total RNA was extracted and used to measure the relative expression levels of selected M1 markers by qPCR. Cell supernatants collected were analyzed for pro-inflammatory cytokine production (TNFα and IL-6) by ELISA.

Expression levels of *CCL2, TNFα, IL-12*, *IL-1β, RelA*, and *SOCS3* were measured using qPCR. While up-regulation of *CCL2, TNFα,* and *IL-1β* was evident in response to IFNγ + 20 pg/ml LPS, we did not observe a significant up-regulation of *IL-12*, *RelA*, and *SOCS3* in response to the lower concentration of LPS in these experiments. NMP-exposure did not affect the response to M1 stimulation (Figure 4.17), with the exception of PVC treatment which inhibited *IL-12* expression in the M1 polarized macrophages (Figure 4.17 (c)-(f)). Thus, for the most part, NMP's exposure did not affect the expression of M1 marker genes in response to M1 polarization.

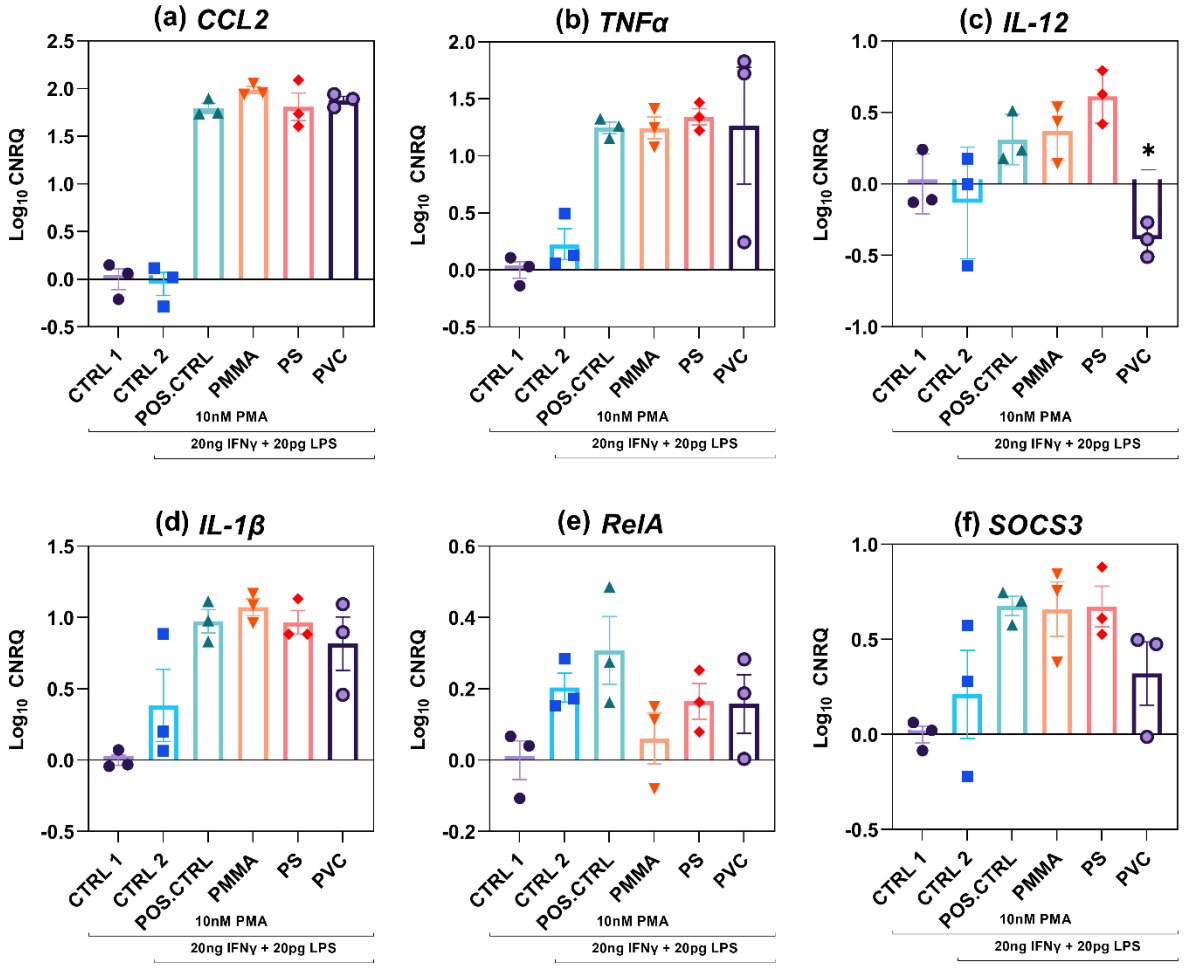

Figure 4.17. Relative expression of M1 macrophage marker genes in macrophages exposed to NMP's during M1 polarization. THP-1 derived macrophages were exposed to different NMP's along with 20 ng/ml IFNγ and 20 pg/ml LPS for 16 h. Relative expression levels of M1 macrophage marker genes were measured by qPCR for **(a)** *CCL2* **(b)** *TNFα* **(c)** *IL-12* **(d** *IL-1β* **(e)** *RelA* and **(f)** *SOCS3*. Data are normalized to three reference genes, and expression is shown relative to vehicle-treated controls (CNRQ) ± SEM. Three independent experiments were performed (n=3). Statistical analysis was carried out with one-way ANOVA in qbase software. CTRL 1 = PBS, CTRL 2 = PBS + 1:10,000 Tween20, POS.CTRL = 20 ng/ml IFNγ + 20 pg/ml LPS. * = $p < 0.05$ compared to the positive control (POS.CTRL)

In the absence of NMP stimulation, we measured an average concentration of 1451 pg/ml TNFα in the positive control. We saw a significant reduction in the TNFα release from the macrophages exposed to all three of the NMP's: 681 pg/ml (PMMA), 742 pg/ml (PS), and 786 pg/ml (PVC) (Figure 4.18 (a)). In the absence of NMP, we measured an average concentration of 88 pg/ml IL-6 concentration in the positive control. Treatment with PS did not affect the IL-6 release, whereas we saw a slight increase in concentrations with response to PVC (98.7 pg/ml) and PMMA (98.3 pg/ml) exposures (Figure 4.18 (b)).

We can conclude that exposure to NMP's suppressed TNFα release in M1 polarized macrophages from the results obtained. In contrast, PMMA and PVC slightly increased the release of IL-6.

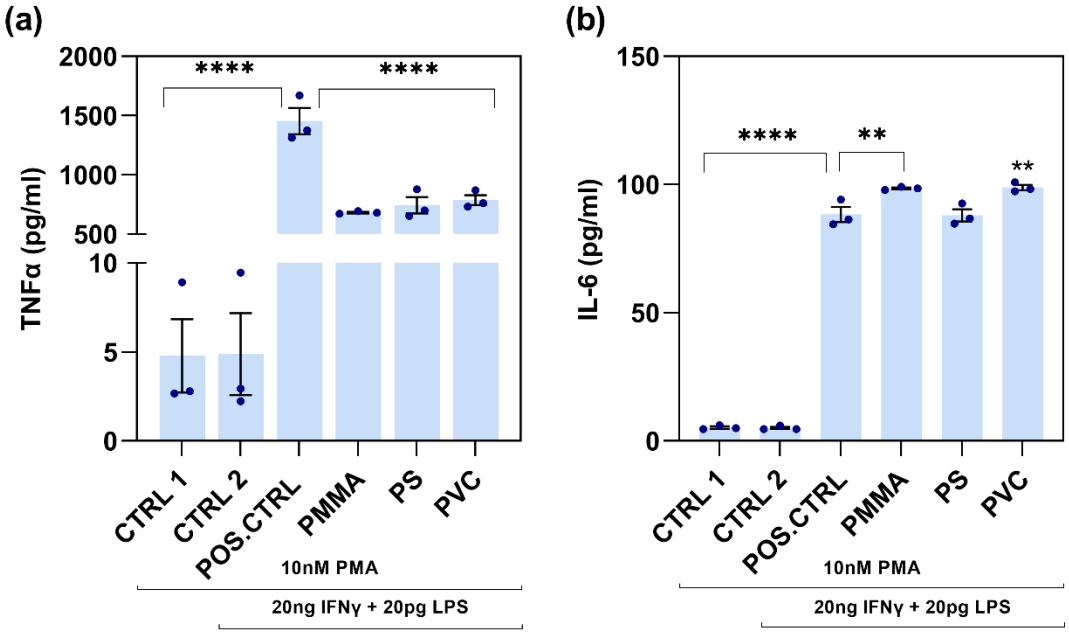

Figure 4.18. Cytokine release in macrophages exposed to NMP during M1 polarization. THP-1 derived macrophages were polarized into M1 macrophage with 20 ng/ml IFNγ and 20 pg/ml LPS in the presence of PMMA, PS or PVC at the highest particle concentrations for 16 h. Cytokine levels in the supernatants were measured by ELISA for **(a)** TNFα and **(b)** IL-6. Results are represented as concentration (pg/ml) mean ± SEM for three biological replicates (n=3). Statistical analysis was performed with one-way ANOVA using GraphPad Prism. CTRL 1 = PBS, CTRL 2 = PBS + 1:10,000 Tween20, POS.CTRL = 20 ng/ml IFNγ + 20 pg/ml LPS. ** = p <0.01, **** = p <0.0001 compared to the positive control (POS.CTRL)

In parallel, we tested the effect of NMP's on cytokine release in macrophages stimulated with 20 ng/ml IFNγ in the absence of LPS. Supernatants from macrophages treated with 20 ng/ml IFNγ (positive control) had an average of 80 pg/ml TNFα; exposure to PMMA, PS, PVC suppressed the IFN-induced TNFα secretion to 8 pg/ml, 7.5 pg/ml, and 13 pg/ml respectively, which was at the borderline of detection for this assay. The level of secreted IL-6 was 80 pg/ml in the positive control, whereas NMP exposed cells produced less IL-6 with 6 pg/ml (in PMMA and PS) and 8.5 pg/ml (in PVC), also at the borderline of detection for this assay. The results in Figure 4.19 (a) and (b) show that the NMP exposure significantly suppresses TNFα and IL-6 cytokines in IFNγ stimulated macrophages.

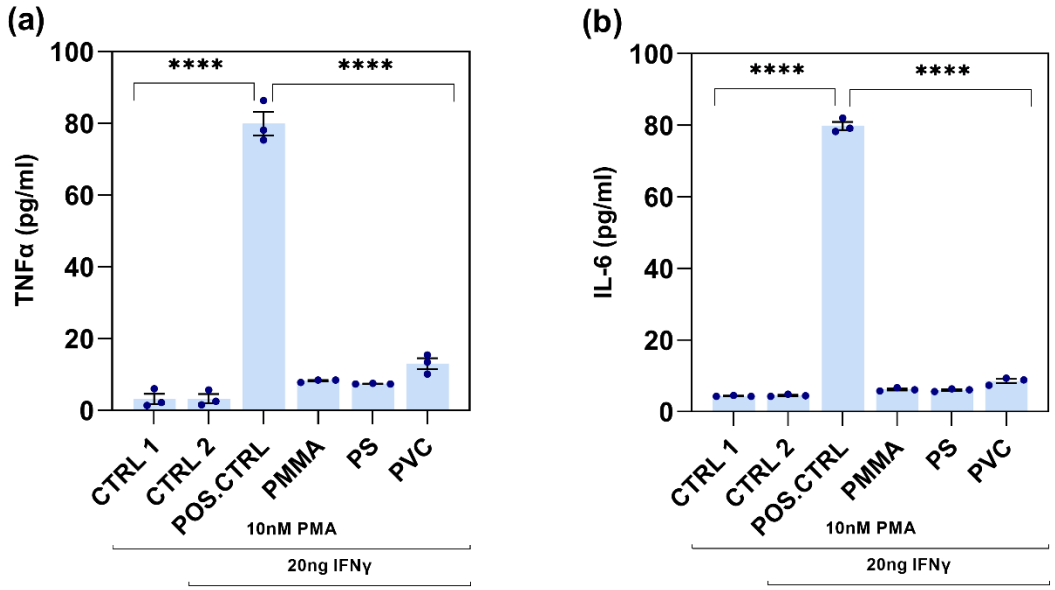

Figure 4.19. Cytokine release in macrophages exposed to NMP during M1 polarization without LPS. Macrophages were treated with 20 ng/ml IFNγ in the presence of PMMA, PS, or PVC at the highest particle concentrations for 16 h. Cytokine release was measured by ELISA for **(a)** TNFα and **(b)** IL-6. Data shown are mean ± SEM of three biological replicates (n=3). One-way ANOVA was performed using GraphPad Prism. CTRL 1 = PBS, CTRL 2 = PBS + 1:10,000 Tween20, POS.CTRL = 20 ng/ml IFNγ. **** = $p < 0.0001$ compared to the positive control (POS.CTRL)

4.5. Investigating whether NMP's exposure cause inflammatory responses in THP-1 monocytes

Monocytes are a subset of cells, a part of the mononuclear phagocyte system, that can differentiate into dendritic cells (DCs) and macrophages. By responding to an inflammatory stimulus, monocytes circulating in the bloodstream as precursor cells migrate into tissues and differentiate into macrophages or DCs [90].

4.5.1. Effect of NMP's in unstimulated THP-1 monocytes

In previous studies with human monocytes isolated from PBMCs, NMP exposure (18 h) triggered both pro and anti-inflammatory cytokines (Weber et al. unpublished data).

We, therefore, wanted to test whether a similar inflammatory response could be triggered by exposure of THP-1 cells to NMP's We exposed the THP-1 cells to the highest concentration of NMP's. After 18 h, supernatants were collected and tested for TNFα, IL-6, and IL-10 cytokines by ELISA.

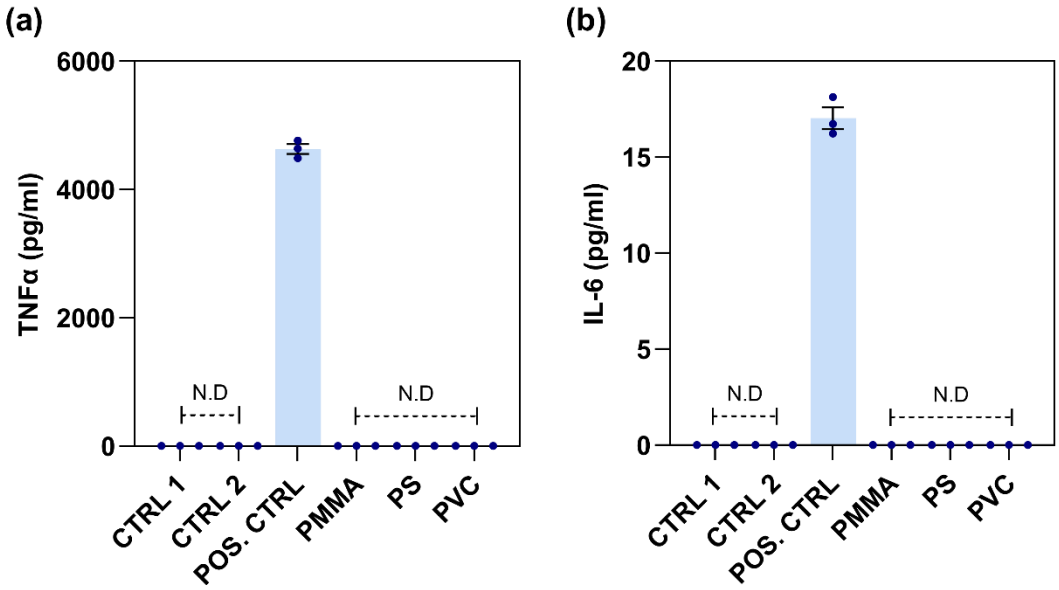

Figure 4.20. Cytokine release in monocytes when exposed to NMP's. THP-1 monocytes were treated with different NMP's at high concentrations for 18 h. Cytokine levels of **(a)** TNFα and **(b)** IL-6 were measured by ELISA. Results are presented as mean calculated concentration (pg/ml) ± SEM with three biological replicates (n=3). Statistical analysis was not performed as concentrations were detected only in the positive control. CTRL 1 = PBS, CTRL 2 = PBS + 1:10,000 Tween20, POS.CTRL = 100 ng/ml LPS.

The concentration of TNFα was 4629 pg/ml, and IL-6 was 17 pg/ml in the LPS-treated monocytes (positive control, Figure 4.20 (a) and (b)). Both cytokines were not detectable in the negative controls and NMP-exposed monocytes. We were unable to detect IL-10, which is considered to be anti-inflammatory and associated with M2 polarization, in any of the samples.

We thus conclude that NMP exposure did not trigger an inflammatory response in THP-1 monocytes or cause the production of IL-10, which is associated with M2 polarization.

4.5.2. Effect of NMP's in LPS stimulated THP-1 monocytes

The results above showed that the NMP exposure did not trigger an inflammatory response in unstimulated monocytes. We, therefore, investigated whether exposure to NMP could affect the inflammatory response triggered with LPS stimulation. To do this, we first determined the EC20 of LPS stimulated TNFα release to ensure that the system was not saturated. To find EC20, we performed an LPS dose-response with varied concentrations from 1 pg/ml to 1 µg/ml, treated for 18 h. The cell supernatants were analyzed for TNFα cytokine release by ELISA.

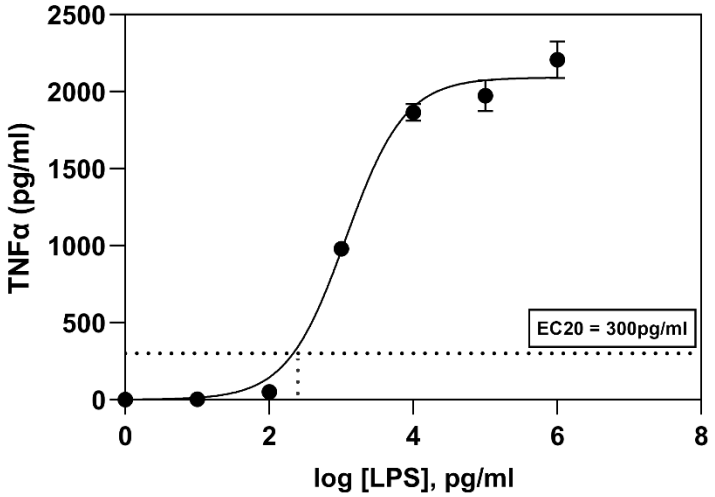

Figure 4.21 Dose-dependent release of TNFα in response to LPS. Monocytes were treated with different LPS concentrations for 18 h. Cell supernatants were harvested and analyzed for TNFα cytokine release by ELISA. Non-linear regression was used to fit the data to a curved and determine the EC20. Data are the mean ± SEM of three technical replicates.

We observed a detectable and dose-dependent release of TNFα in response to LPS in between 1 pg/ml and 1μg/ml. EC20 was calculated as 300 pg/ml (Figure 4.21) (refer to section 3.10).

THP-1 monocytes were thus treated with 300 pg/ml LPS in the presence or absence of NMP's for 18 h. Supernatants were analyzed for TNFα, IL-6, and IL-10 production by ELISA.

In the absence of NMP exposure, the TNFα concentration was 223 pg/ml in the positive control. We saw a significant reduction in TNFα release from the LPS stimulated macrophages exposed to all three NMP's: 100 pg/ml (PMMA), 88 pg/ml (PS), and 115 pg/ml (PVC) ((Figure 4.22 (a)). In the absence of NMP exposure, the IL-6 concentration was 78 pg/ml in the positive control. In cells treated with NMP's, the concentrations were 4 pg/ml, which is below the assay's detection limit (Figure 4.22 (b)). We were unable to detect IL-10, which is considered to be anti-inflammatory.

We thus conclude that the NMP exposure suppresses TNFα and IL-6 cytokines signaling in LPS stimulated monocytes.

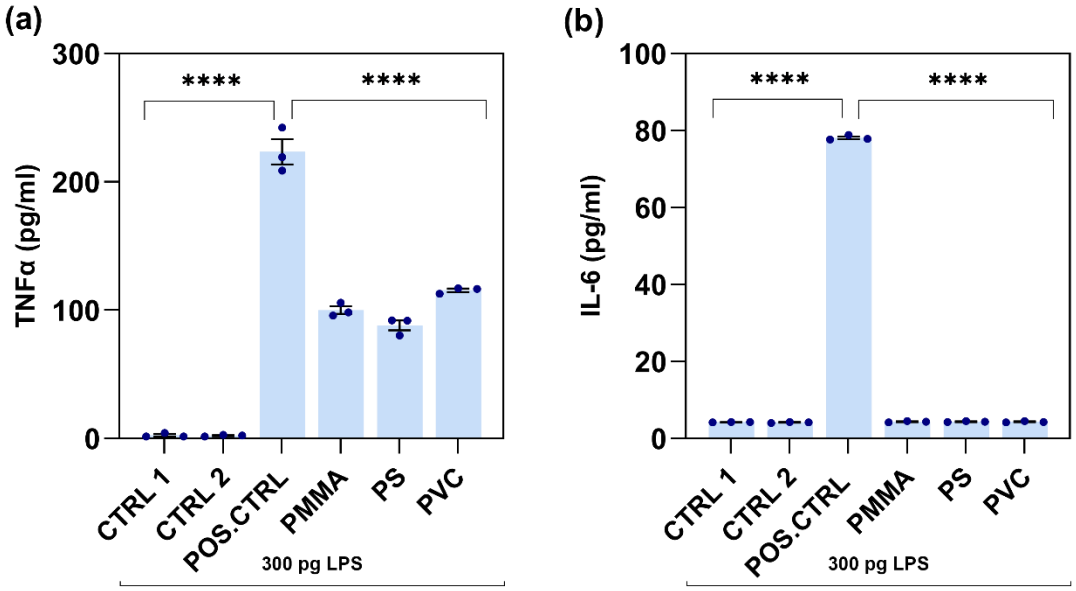

Figure 4.22. Cytokine profiling in LPS-stimulated THP-1 monocytes exposed to NMP's. LPS-treated monocytes were exposed to different NMP's at high concentrations. Cell supernatants collected by 18 h were measured for cytokine release in LPS-stimulated monocytes as shown **(a)** TNFα (**b)** IL-6. Results are shown as calculated mean concentration (pg/ml) ± SEM with three biological replicates (n=3). By one-way ANOVA, statistical analysis was performed using GraphPad software. CTRL 1 = PBS, CTRL 2 = PBS + 1:10,000 Tween20, POS.CTRL =300 pg/ml LPS. **** = p <0.0001 compared to the positive control (POS.CTRL)

5 Discussion

This master thesis aims to investigate whether NMP's have pro-inflammatory effects in monocytes or macrophages using the THP-1 cell line as a model. Using confocal microscopy and different approaches to measure inflammatory responses, we were able to conclude that the NMP's made of PMMA, PS, and PVC sources were recognized and internalized by macrophages but did not have pro-inflammatory effects under these experimental conditions.

5.1 Cytotoxicity

Any particulate which is foreign to our body can exhibit a toxic effect [91]. Microplastics entering the human body may cause toxicity, followed by inducing or enhancing an inflammatory response [7]. Based on the polymer type, the toxicity may vary based on several factors like size, concentration, charge, and shape [92] and show differential cytotoxic effects in cell types [93]. Therefore, it was essential to assess if the NMP's we used in this study affect the THP-1 cell viability. Thus, we investigated the cytotoxicity of PMMA, PS, and PVC plastic particles with different concentrations in monocytes and macrophages for short and long-time exposure.

The cytotoxic effects of PS in immune cells were previously investigated by Lunov et al. [85]. They reported that neither carboxy nor amino-functionalized spherical PS nanoparticles (0.01-100 μg/ml) had any effect on cell viability in THP-1 monocytes and macrophages following 48 h of exposure. In contrast, we showed that exposure to the irregular polydisperse PS at the highest concentration (≈ 0.5 μg/ml) caused a slight reduction in monocyte viability after 24 h. Interestingly, we observed reduced viability after 72 h exposure to PS in both monocytes and macrophages, together suggesting that cytotoxicity may increase with longer exposure times and supports the use of longer exposure times in future studies.

The cytotoxicity of PMMA on human-monocyte-derived macrophages was investigated by Yoshioka et al. [94]. They reported decreased cell viability after 24 h exposure to PMMA beads at a concentration of 1000 particles/cell. In contrast, we did not see any effect of the polydisperse PMMA in monocytes or macrophages after 24 h. We did, however, show a reduced viability of macrophages after 72 h of exposure. The primary macrophages may be more sensitive to the cytotoxic effects of PMMA compared to THP-1 derived macrophages, or given that particles of different sizes and shapes can have differing cytotoxic properties, their use of uniform beads versus polydisperse PMMAs may also be important.

Polydisperse PVC microplastics with concentrations ranging from 10-1000 μg/ml were previously shown to not affect the viability of PBMCs after 24 h of exposure [95]. Our findings in THP-1 monocytes agree with and expand on this study to show PVC was not cytotoxic at concentrations of ca. 4 μg/ml-25 mg/ml up to an exposure duration of 72 h. Interestingly, PVC was toxic at the concentration of ca. 25 mg/ml in the THP-1-derived macrophages after 72 h of exposure. While we were unable to find any studies investigating the cytotoxicity of PVC particles specifically in macrophages. Mahadevan et al. [96] reported a high toxicity of PVC beads at 200 μg/ml in non-immune cells (BHK-1 cells) after 72 h.

5.2 Particle internalization

The internalization of NMP's by macrophages has been demonstrated previously for PMMA [97], [98], and PS [13] [85]. Using live confocal microscopy, we demonstrated that THP-1 derived macrophages fully internalized polydisperse PMMA, PS, and PVC particles within 16 h of exposure. We investigated internalization using both live imaging and in fixed cells. While we saw internalization at 30 min in the fixed cells, the particles we observed in the live cells appeared to be adhered to the cells but not internalized at this time point. It was unclear if this was due to differences in the handling of the cells, or the increased accuracy achieved by imaging the plasma membrane stain in living cells.

Papa et al. [98] reported that *in vivo*, microglial cells stimulated with LPS internalized PMMA beads within 30 min of exposure, which rather agrees with findings in the fixed cells. The internalization of functionalized PS (PS-COOH) particles in THP-1 macrophages after 2 h and 24 h of exposure, were previously reported by Lunov et al. [85] and Stock et al. [13]. We were unable to find studies demonstrating the specific internalization of PVC by macrophages. A study using Caco-2 cells, exposed to irregular PVC particles for 24 h, reported there was almost no cell contact [99], implying that the uptake of the PVC may require mechanisms specific to phagocytic cell types.

Thus, we demonstrated that THP-1 derived macrophages internalized NMPs, but, as discussed below, our data suggested that this did not produce an inflammatory response under these experimental conditions and could, in fact, suppress some responses to pro-inflammatory stimuli. Phagocytosis occurs in a complex manner that involves many diverse cellular processes to ingest the foreign particles and illicit the appropriate immune response [100]. Mechanisms of particle

internalization depend on the type of receptors that recognize the particulates and the characteristics of the particle itself. The variable mechanisms of phagocytosis have strong effects on the inflammatory response [101]. For example, phagocytosis mediated by the complement receptor does not typically cause inflammation versus phagocytosis mediated by the Fc receptor, which is highly pro-inflammatory, and the internalization of apoptotic cells is generally anti-inflammatory [102, 103]. Endocytic mechanisms are also triggered by a huge spectrum of pattern recognition receptors (PRRs) which recognize specific pathogens and foreign matter and typically result in an inflammatory response [104], while non-receptor mediated endocytosis mediated by the clathrin-coat assembly, or macro-pinocytosis, for example, may not be pro-inflammatory [105].

5.3 NMP exposure and inflammatory effects in macrophages

Based on previous observations of the general effects of NMP's on immune responses [66, 94, 106, 107] and on our own studies with the polydisperse NMP's used here (Weber et al. unpublished). We hypothesized that the internalization of NMP's by the THP-1 derived macrophages would trigger pro-inflammatory responses.

Activation of NF-κB is common to many pro-inflammatory stimuli [88] and is required for phagocytosis of certain pathogens [108]. NF-κB has been implicated in the cytotoxic response to PS NMP's in epithelial cells, but the effects in immune cells have, to my knowledge, not been explored [109]. We report here that none of the three NMP types activated NF-κB (up to 24 h) in macrophages. A similar study was performed by Toshihiro et al. [110], where they tested the isolated titanium-alloy particles (known as particle wear debris) from a human total hip arthroplasty in THP-1 macrophages for NF-κB activation. The results demonstrated that with LPS-treated particles, translocation of NF-κB was seen, whereas the particles alone were not capable of activating NF-κB. This study was in agreement with our findings, despite the different particle type.

Consistent with established methods, treatment of THP-1 macrophages with IFNγ + LPS caused polarization to a pro-inflammatory (M1) phenotype associated with upregulation of expression of M1 macrophage genes and secretion of pro-inflammatory cytokines TNFα and IL-6. Supporting the lack of NF-κB activation shown previously, but in contrast to our hypothesis, exposure to the

NMP's had no effect on the expression of M1 marker genes or on the release of TNFα or IL-6. Previous studies reported an induction of pro-inflammatory cytokines in THP-1 macrophages exposed to carboxylated PS particles (20 μg/ml) and showed an increased IL-6 secretion by 24 h [66]. Carboxylation of particles may alter the mechanism or degree of uptake, and the studies used higher concentrations of PS which may account for the discrepancy between the findings. PMMA beads were also reported to cause the production of TNFα and IL-6 cytokines in human-monocyte-derived macrophages after 24 h. [94] . In this case, the beads were not modified. However, the use of macrophages derived from primary monocytes is an important difference between this study and ours, given that we previously showed pro-inflammatory effects of similar polydisperse nanoparticles in primary immune cells (Weber et al. unpublished), we suggest the origin of the macrophages may be an important determinant of the cellular response.

5.4 Exposure to NMP's during M1 polarization

Exposure to NMP's during M1 polarization did not alter the induction of *CCL2* or *TNFα* expression. Stock et al. [13] reported a similar lack of effect of functionalized PS particles on macrophage polarization. They exposed THP-1 macrophages to PS particles at concentrations 25,000, 60,000, and 100,000 particles/ml for 24 h, followed by M1 and M2 stimulation for 30 min, 24 h, and 72 h, and showed that the expression levels of M1 or M2 specific surface receptors and chemokines (*CD206, CD209, CCL22*, and *CXCL10*) were not affected.

In contrast to the gene expression data, we showed that exposure to all three NMP types suppressed the release of TNFα during M1 polarization. Fuchs et al. [111] reported that M1 macrophages obtained from PBMCs exposed to functionalized PS particles in for 6 h did not affect the TNFα cytokine release during M1 polarization, which was not in agreement with our results. However, the shorter time duration, different particle types, and different macrophage origins make it difficult to compare this data with our findings. When we removed the LPS stimulation during M1 polarization, NMP exposures strongly suppressed the TNFα and IL-6 cytokine production. To our knowledge, no previous studies have been reported the effects of plastic exposure during M1 polarization using IFNγ alone.

5.5 NMP exposure and inflammatory effects in monocytes

We previously showed that PMMA, PS, and PVC particles caused pro-inflammatory cytokines release in human monocytes (Weber et al. unpublished). Based on this finding, we hypothesized

that a similar response would be observed in THP-1 cells, as they are used as an *in vitro* cell model for human monocytes [54, 112].

However, when we exposed the THP-1 cells to PMMA, PS, and PVC NMP's we did not see any release of TNFα, IL-6, or IL-10. Our results were in contrast with studies by Prietl et al. [66], who reported that carboxylated PS particles promoted IL-6 cytokine production in THP-1 monocytes after 24 h of exposure. Han et al. [95] used longer exposure times (4 days) but also reported the production of cytokines (TNFα and IL-6) in response to microplastics. They used polydisperse PVC microplastics with concentrations ranging from 10-1000 μg/ml in PBMCs. Interestingly, the TNFα induction decreased with increased concentrations of PVC.

When we stimulated the THP-1 cells with LPS, NMP's suppressed TNFα and IL-6 release, which was in contrast with Schutte et al. [113] who tested PMMA, and PVC particles in LPS treated THP-1 monocytes for 24 h and reported an induction of TNFα, and IL-10 but not of IL-6. The suppression of TNFα and IL-6 response to LPS, independent of polymer type, has been previously shown for non-plastic nanoparticles, but it is unclear what mechanisms may be involved [114, 115].

6 Conclusion and future perspective

The biological response of the immune cells to the secondary NMP's is not well understood. There is some evidence that certain types of NMP's can trigger inflammation through their interactions with immune cells [4, 94, 95, 113]. The main aim of this thesis was to investigate, using the THP-1cell line, whether an inflammatory response is activated when monocytes and macrophages are exposed to polydisperse secondary NMP's made of PMMA, PS, and PVC.

To summarize the results, the nanoparticle tracking analysis showed that the sizes of the NMP's were in the range of 70-600 nm. Particle analysis by confocal microscopy demonstrated a predominance of larger particles (or aggregated particles) at the bottom of the culture wells. All polymer types tested were internalized by the macrophages. Cytotoxicity resulting from NMP exposure varied between polymer types but was more evident after longer exposure times. NMP exposures did not activate NF-κB or polarize the macrophages toward a pro-inflammatory (M1) phenotype and did not cause inflammatory cytokine release in either monocytes or macrophages. Instead, NMP exposure during monocyte or macrophage activation suppressed the release of inflammatory cytokines.

Given that our results do not support the studies carried out using the same polydisperse polymer types in primary immune cells, it will be important to repeat this study using primary human monocytes and macrophages in parallel to assess the feasibility of using THP-1 cells as a model system for studying effects of NMP's on immune cells. Also, although our findings appear to be generally inconsistent with the published literature, it is common that studies with negative findings are underreported, so it is difficult to make a good comparison.

However, our data suggest that in THP-1 cells, the internalization of polydisperse NMP's does not initiate inflammatory activation of monocytes or macrophages, suggesting a lack of FcR or PRR involvement. It would be interesting to explore the uptake mechanisms involved in the internalization of these NMP's and investigate this in both primary and THP-1 differentiated macrophages. Such a comparative study could help to understand the differences in the inflammatory responses observed between the two cell types.

While our studies accurately determined that the macrophages were able to internalize the NMPs, a clear limitation was that we made no attempt to quantify either number of cells with internalized

NMP's, the numbers of particles internalized, or the size distribution of the internalized particles. Since previous studies have reported that varying sizes could also influence the inflammatory response, addressing this limitation would be an important future goal. Our studies were often also limited by the use of single time points and single exposure concentrations. Including longer exposures and NMP's dose-response studies would allow for more confidence in the data.

We would also propose investigating effects on other monocyte and macrophage activation states (e.g., M2 polarization). One study reported suppression of IL-10 by NMP's in M2 macrophages [111], while monocytes and other reported induction of IL-10 release [113]. Understanding the risks associated with NMPs exposures will require a detailed understanding of how these particles are recognized and internalized by different types of cells. Given the diversity and complexity of secondary NMPs and the diversity of immune cells and immune cell activation states, this becomes a significant challenge that should be addressed.

7 References

1. Zalasiewicz, J., et al., *The geological cycle of plastics and their use as a stratigraphic indicator of the Anthropocene.* Anthropocene, 2016. **13**: p. 4-17.
2. Jambeck, J.R., et al., *Marine pollution. Plastic waste inputs from land into the ocean.* Science, 2015. **347**(6223): p. 768-71.
3. Geyer, R., J.R. Jambeck, and K.L. Law, *Production, use, and fate of all plastics ever made.* Sci Adv, 2017. **3**(7): p. e1700782.
4. Yong, C.Q.Y., S. Valiyaveetill, and B.L. Tang, *Toxicity of Microplastics and Nanoplastics in Mammalian Systems.* Int J Environ Res Public Health, 2020. **17**(5).
5. Hartmann, N.B., et al., *Are We Speaking the Same Language? Recommendations for a Definition and Categorization Framework for Plastic Debris.* Environ Sci Technol, 2019. **53**(3): p. 1039-1047.
6. Lambert, S. and M. Wagner, *Formation of microscopic particles during the degradation of different polymers.* Chemosphere, 2016. **161**: p. 510-517.
7. Wright, S.L. and F.J. Kelly, *Plastic and Human Health: A Micro Issue?* Environ Sci Technol, 2017. **51**(12): p. 6634-6647.
8. Chain, E.Panel o.C.i.t.F., *Presence of microplastics and nanoplastics in food, with particular focus on seafood.* EFSA Journal, 2016. **14**(6): p. e04501.
9. Napper, I.E., et al., *Characterisation, quantity and sorptive properties of microplastics extracted from cosmetics.* Marine Pollution Bulletin, 2015. **99**(1): p. 178-185.
10. van Wezel, A., I. Caris, and S.A.E. Kools, *Release of primary microplastics from consumer products to wastewater in the Netherlands.* Environmental Toxicology and Chemistry, 2016. **35**(7): p. 1627-1631.
11. Cole, M., et al., *Microplastics as contaminants in the marine environment: A review.* Marine Pollution Bulletin, 2011. **62**(12): p. 2588-2597.
12. Hirt, N. and M. Body-Malapel, *Immunotoxicity and intestinal effects of nano- and microplastics: a review of the literature.* Part Fibre Toxicol, 2020. **17**(1): p. 57.
13. Stock, V., et al., *Uptake and effects of orally ingested polystyrene microplastic particles in vitro and in vivo.* Arch Toxicol, 2019. **93**(7): p. 1817-1833.
14. Barboza, L.G.A., et al., *Marine microplastic debris: An emerging issue for food security, food safety and human health.* Marine Pollution Bulletin, 2018. **133**: p. 336-348.
15. Lusher, A., p. hollman, and J. Mendoza, *Microplastics in fisheries and aquaculture: Status of knowledge on their occurrence and implications for aquatic organisms and food safety*. 2017.
16. Yee, M.S.-L., et al., *Impact of Microplastics and Nanoplastics on Human Health.* Nanomaterials, 2021. **11**(2): p. 496.
17. Carr, K.E., et al., *Morphological aspects of interactions between microparticles and mammalian cells: intestinal uptake and onward movement.* Prog Histochem Cytochem, 2012. **46**(4): p. 185-252.
18. Harmsen, A.G., et al., *The role of macrophages in particle translocation from lungs to lymph nodes.* Science, 1985. **230**(4731): p. 1277-80.
19. Oberdörster, G., et al., *Increased pulmonary toxicity of ultrafine particles? II. Lung lavage studies.* Journal of Aerosol Science, 1990. **21**(3): p. 384-387.
20. Kohli, A.K. and H.O. Alpar, *Potential use of nanoparticles for transcutaneous vaccine delivery: effect of particle size and charge.* Int J Pharm, 2004. **275**(1-2): p. 13-7.

21. Mahe, B., et al., *Nanoparticle-based targeting of vaccine compounds to skin antigen-presenting cells by hair follicles and their transport in mice.* J Invest Dermatol, 2009. **129**(5): p. 1156-64.
22. Eyles, J.E., et al., *Microsphere translocation and immunopotentiation in systemic tissues following intranasal administration.* Vaccine, 2001. **19**(32): p. 4732-42.
23. Jani, P., et al., *The uptake and translocation of latex nanospheres and microspheres after oral administration to rats.* J Pharm Pharmacol, 1989. **41**(12): p. 809-12.
24. Chakrabarty, G., M. Vashishtha, and D. Leeder, *Polyethylene in knee arthroplasty: A review.* Journal of clinical orthopaedics and trauma, 2015. **6**(2): p. 108-112.
25. Anderson, J.C., B.J. Park, and V.P. Palace, *Microplastics in aquatic environments: Implications for Canadian ecosystems.* Environ Pollut, 2016. **218**: p. 269-280.
26. Smith, M., et al., *Microplastics in Seafood and the Implications for Human Health.* Curr Environ Health Rep, 2018. **5**(3): p. 375-386.
27. Prame Kumar, K., A.J. Nicholls, and C.H.Y. Wong, *Partners in crime: neutrophils and monocytes/macrophages in inflammation and disease.* Cell and Tissue Research, 2018. **371**(3): p. 551-565.
28. Aristizábal, B., *"Innate Immune System." Autoimmunity: From Bench to Bedside [Internet]*. 2013.
29. van Furth, R. and Z.A. Cohn, *The origin and kinetics of mononuclear phagocytes.* J Exp Med, 1968. **128**(3): p. 415-35.
30. Geissmann, F., et al., *Development of monocytes, macrophages, and dendritic cells.* Science, 2010. **327**(5966): p. 656-61.
31. Chiu, S. and A. Bharat, *Role of monocytes and macrophages in regulating immune response following lung transplantation.* Current opinion in organ transplantation, 2016. **21**(3): p. 239-245.
32. Yang, J., et al., *Monocyte and macrophage differentiation: circulation inflammatory monocyte as biomarker for inflammatory diseases.* Biomarker research, 2014. **2**(1): p. 1-1.
33. Ziegler-Heitbrock, L., et al., *Nomenclature of monocytes and dendritic cells in blood.* Blood, 2010. **116**(16): p. e74-80.
34. Mukherjee, R., et al., *Non-Classical monocytes display inflammatory features: Validation in Sepsis and Systemic Lupus Erythematous.* Sci Rep, 2015. **5**: p. 13886.
35. Al Dubayee, M.S., et al., *Differential Expression of Human Peripheral Mononuclear Cells Phenotype Markers in Type 2 Diabetic Patients and Type 2 Diabetic Patients on Metformin.* Frontiers in endocrinology, 2018. **9**: p. 537-537.
36. Gordon, S., *Pattern recognition receptors: doubling up for the innate immune response.* Cell, 2002. **111**(7): p. 927-30.
37. Hume, D.A., *Macrophages as APC and the dendritic cell myth.* J Immunol, 2008. **181**(9): p. 5829-35.
38. Wynn, T.A., A. Chawla, and J.W. Pollard, *Macrophage biology in development, homeostasis and disease.* Nature, 2013. **496**(7446): p. 445-55.
39. Hussell, T. and T.J. Bell, *Alveolar macrophages: plasticity in a tissue-specific context.* Nature Reviews Immunology, 2014. **14**(2): p. 81-93.
40. Murray, P.J., et al., *Macrophage activation and polarization: nomenclature and experimental guidelines.* Immunity, 2014. **41**(1): p. 14-20.
41. Ghosh, S. and M. Karin, *Missing pieces in the NF-kappaB puzzle.* Cell, 2002. **109 Suppl**: p. S81-96.

42. Barnes, P.J. and M. Karin, *Nuclear factor-kappaB: a pivotal transcription factor in chronic inflammatory diseases.* N Engl J Med, 1997. **336**(15): p. 1066-71.
43. Tripathi, P. and A. Aggarwal, *NF-kB transcription factor: a key player in the generation of immune response.* Current Science, 2006. **90**(4): p. 519-531.
44. Tsuchiya, S., et al., *Establishment and characterization of a human acute monocytic leukemia cell line (THP-1).* Int J Cancer, 1980. **26**(2): p. 171-6.
45. Kramer, P.R. and S. Wray, *17-β-Estradiol regulates expression of genes that function in macrophage activation and cholesterol homeostasis.* The Journal of Steroid Biochemistry and Molecular Biology, 2002. **81**(3): p. 203-216.
46. Tsuchiya, S., et al., *Induction of maturation in cultured human monocytic leukemia cells by a phorbol diester.* Cancer Res, 1982. **42**(4): p. 1530-6.
47. Chanput, W., et al., *beta-Glucans are involved in immune-modulation of THP-1 macrophages.* Mol Nutr Food Res, 2012. **56**(5): p. 822-33.
48. Chanput, W., J.J. Mes, and H.J. Wichers, *THP-1 cell line: an in vitro cell model for immune modulation approach.* International immunopharmacology, 2014. **23**(1): p. 37-45.
49. Chanput, W., et al., *Characterization of polarized THP-1 macrophages and polarizing ability of LPS and food compounds.* Food Funct, 2013. **4**(2): p. 266-76.
50. Daigneault, M., et al., *The identification of markers of macrophage differentiation in PMA-stimulated THP-1 cells and monocyte-derived macrophages.* PLoS One, 2010. **5**(1): p. e8668.
51. Schwende, H., et al., *Differences in the state of differentiation of THP-1 cells induced by phorbol ester and 1,25-dihydroxyvitamin D3.* J Leukoc Biol, 1996. **59**(4): p. 555-61.
52. Phillips, R.J., M. Lutz, and B. Premack, *Differential signaling mechanisms regulate expression of CC chemokine receptor-2 during monocyte maturation.* Journal of Inflammation, 2005. **2**(1): p. 14.
53. Takahashi, K., *Development and Differentiation of Macrophages and Related Cells Historical Review and Current Concepts.* Journal of Clinical and Experimental Hematopathology, 2001. **41**(1): p. 1-31.
54. Auwerx, J., *The human leukemia cell line, THP-1: a multifacetted model for the study of monocyte-macrophage differentiation.* Experientia, 1991. **47**(1): p. 22-31.
55. Gatto, F., et al., *PMA-Induced THP-1 Macrophage Differentiation is Not Impaired by Citrate-Coated Platinum Nanoparticles.* Nanomaterials (Basel, Switzerland), 2017. **7**(10): p. 332.
56. Gordon, S., *Alternative activation of macrophages.* Nature Reviews Immunology, 2003. **3**(1): p. 23-35.
57. Mosser, D.M. and J.P. Edwards, *Exploring the full spectrum of macrophage activation.* Nature Reviews Immunology, 2008. **8**(12): p. 958-969.
58. Mantovani, A., et al., *Macrophage polarization: tumor-associated macrophages as a paradigm for polarized M2 mononuclear phagocytes.* Trends in Immunology, 2002. **23**(11): p. 549-555.
59. Nakanishi, Y., et al., *COX-2 inhibition alters the phenotype of tumor-associated macrophages from M2 to M1 in Apc Min/+ mouse polyps.* Carcinogenesis, 2011. **32**(9): p. 1333-1339.
60. Cheng, X., et al., *Adiponectin Induces Pro-inflammatory Programs in Human Macrophages and CD4+ T Cells.* Journal of Biological Chemistry, 2012. **287**(44): p. 36896-36904.

61. Mosmann, T.R., et al., *Two types of murine helper T cell clone. I. Definition according to profiles of lymphokine activities and secreted proteins.* J Immunol, 1986. **136**(7): p. 2348-57.
62. Mantovani, A., et al., *The chemokine system in diverse forms of macrophage activation and polarization.* Trends Immunol, 2004. **25**(12): p. 677-86.
63. Bezold, V., et al., *Glycation of macrophages induces expression of pro-inflammatory cytokines and reduces phagocytic efficiency.* Aging, 2019. **11**(14): p. 5258-5275.
64. Shiratori, H., et al., *THP-1 and human peripheral blood mononuclear cell-derived macrophages differ in their capacity to polarize in vitro.* Molecular Immunology, 2017. **88**: p. 58-68.
65. Deng, Y., et al., *Tissue accumulation of microplastics in mice and biomarker responses suggest widespread health risks of exposure.* Scientific Reports, 2017. **7**(1): p. 46687.
66. Prietl, B., et al., *Nano-sized and micro-sized polystyrene particles affect phagocyte function.* Cell Biol Toxicol, 2014. **30**(1): p. 1-16.
67. Magrì, D., et al., *Laser Ablation as a Versatile Tool To Mimic Polyethylene Terephthalate Nanoplastic Pollutants: Characterization and Toxicology Assessment.* ACS Nano, 2018. **12**(8): p. 7690-7700.
68. Hesler, M., et al., *Multi-endpoint toxicological assessment of polystyrene nano- and microparticles in different biological models in vitro.* Toxicol In Vitro, 2019. **61**: p. 104610.
69. Dong, C.-D., et al., *Polystyrene microplastic particles: In vitro pulmonary toxicity assessment.* Journal of Hazardous Materials, 2020. **385**: p. 121575.
70. Xu, M., et al., *Internalization and toxicity: A preliminary study of effects of nanoplastic particles on human lung epithelial cell.* Science of The Total Environment, 2019. **694**: p. 133794.
71. Hwang, J., et al., *An assessment of the toxicity of polypropylene microplastics in human derived cells.* Sci Total Environ, 2019. **684**: p. 657-669.
72. Filipe, V., A. Hawe, and W. Jiskoot, *Critical Evaluation of Nanoparticle Tracking Analysis (NTA) by NanoSight for the Measurement of Nanoparticles and Protein Aggregates.* Pharmaceutical Research, 2010. **27**(5): p. 796-810.
73. Carpenter, A.E., et al., *CellProfiler: image analysis software for identifying and quantifying cell phenotypes.* Genome Biol, 2006. **7**(10): p. R100.
74. Riss, T.L., et al., *Cell Viability Assays*, in *Assay Guidance Manual*, S. Markossian, et al., Editors. 2004, Eli Lilly & Company and the National Center for Advancing Translational Sciences: Bethesda (MD).
75. Tamminga, M., E. Hengstmann, and E. Fischer, *Nile Red Staining as a Subsidiary Method for Microplastic Quantification: A Comparison of Three Solvents and Factors Influencing Application Reliability.* Journal of Earth Sciences & Environmental Studies, 2017.
76. Trask, O.J., Jr., *Nuclear Factor Kappa B (NF-κB) Translocation Assay Development and Validation for High Content Screening*, in *Assay Guidance Manual*, S. Markossian, et al., Editors. 2004, Eli Lilly & Company and the National Center for Advancing Translational Sciences: Bethesda (MD).
77. Takashiba, S., et al., *Differentiation of monocytes to macrophages primes cells for lipopolysaccharide stimulation via accumulation of cytoplasmic nuclear factor kappaB.* Infect Immun, 1999. **67**(11): p. 5573-8.

78. Noursadeghi, M., et al., *Quantitative imaging assay for NF-kappaB nuclear translocation in primary human macrophages.* Journal of immunological methods, 2008. **329**(1-2): p. 194-200.
79. Ramakers, C., et al., *Assumption-free analysis of quantitative real-time polymerase chain reaction (PCR) data.* Neurosci Lett, 2003. **339**(1): p. 62-6.
80. Hellemans, J., et al., *qBase relative quantification framework and software for management and automated analysis of real-time quantitative PCR data.* Genome Biol, 2007. **8**(2): p. R19.
81. Maess, M.B., S. Sendelbach, and S. Lorkowski, *Selection of reliable reference genes during THP-1 monocyte differentiation into macrophages.* BMC molecular biology, 2010. **11**: p. 90-90.
82. Tanaka, A., et al., *Selection of reliable reference genes for the normalisation of gene expression levels following time course LPS stimulation of murine bone marrow derived macrophages.* BMC immunology, 2017. **18**(1): p. 43-43.
83. Kalagara, R., et al., *Identification of stable reference genes for lipopolysaccharide-stimulated macrophage gene expression studies.* Biology Methods and Protocols, 2016. **1**(1).
84. Huang, X., D.P. Cavalcante, and H.E. Townley, *Macrophage-like THP-1 cells show effective uptake of silica nanoparticles carrying inactivated diphtheria toxoid for vaccination.* Journal of Nanoparticle Research, 2020. **22**(1): p. 23.
85. Lunov, O., et al., *Differential Uptake of Functionalized Polystyrene Nanoparticles by Human Macrophages and a Monocytic Cell Line.* ACS nano, 2011. **5**: p. 1657-69.
86. Kurynina, A.V., et al., *Plasticity of Human THP-1 Cell Phagocytic Activity during Macrophagic Differentiation.* Biochemistry (Mosc), 2018. **83**(3): p. 200-214.
87. Sharif, O., et al., *Transcriptional profiling of the LPS induced NF-kappaB response in macrophages.* BMC Immunol, 2007. **8**: p. 1.
88. Liu, T., et al., *NF-κB signaling in inflammation.* Signal transduction and targeted therapy, 2017. **2**: p. 17023.
89. Genin, M., et al., *M1 and M2 macrophages derived from THP-1 cells differentially modulate the response of cancer cells to etoposide.* BMC Cancer, 2015. **15**(1): p. 577.
90. Teh, Y.C., et al., *Capturing the Fantastic Voyage of Monocytes Through Time and Space.* Front Immunol, 2019. **10**: p. 834.
91. Buzea, C., Pacheco, II, and K. Robbie, *Nanomaterials and nanoparticles: sources and toxicity.* Biointerphases, 2007. **2**(4): p. Mr17-71.
92. Revel, M., A. Châtel, and C. Mouneyrac, *Micro(nano)plastics: A threat to human health?* Current Opinion in Environmental Science & Health, 2018. **1**: p. 17-23.
93. Banerjee, A. and W.L. Shelver, *Micro- and nanoplastic induced cellular toxicity in mammals: A review.* Science of The Total Environment, 2021. **755**: p. 142518.
94. Yoshioka, R., et al., *The biological response of macrophages to PMMA particles with different morphology and size.* Biosurface and Biotribology, 2016. **2**(3): p. 114-120.
95. Han, S., et al., *Surface Pattern Analysis of Microplastics and Their Impact on Human-Derived Cells.* ACS Applied Polymer Materials, 2020. **2**(11): p. 4541-4550.
96. Mahadevan, G. and S. Valiyaveettil, *Understanding the interactions of poly(methyl methacrylate) and poly(vinyl chloride) nanoparticles with BHK-21 cell line.* Sci Rep, 2021. **11**(1): p. 2089.

97. Horowitz, S.M., et al., *Studies of the mechanism by which the mechanical failure of polymethylmethacrylate leads to bone resorption.* J Bone Joint Surg Am, 1993. **75**(6): p. 802-13.
98. Papa, S., et al., *Polymeric Nanoparticle System to Target activated microglia/macrophages in Spinal Cord Injury.* Journal of controlled release : official journal of the Controlled Release Society, 2013. **174**.
99. Stock, V., et al., *Uptake and cellular effects of PE, PP, PET and PVC microplastic particles.* Toxicology in Vitro, 2021. **70**: p. 105021.
100. Rosales, C. and E. Uribe-Querol, *Phagocytosis: A Fundamental Process in Immunity.* BioMed research international, 2017. **2017**: p. 9042851-9042851.
101. Gustafson, H.H., et al., *Nanoparticle Uptake: The Phagocyte Problem.* Nano today, 2015. **10**(4): p. 487-510.
102. Aderem, A. and D.M. Underhill, *Mechanisms of phagocytosis in macrophages.* Annu Rev Immunol, 1999. **17**: p. 593-623.
103. Aderem, A., *Phagocytosis and the inflammatory response.* J Infect Dis, 2003. **187 Suppl 2**: p. S340-5.
104. Mogensen, T.H., *Pathogen recognition and inflammatory signaling in innate immune defenses.* Clinical microbiology reviews, 2009. **22**(2): p. 240-273.
105. Behzadi, S., et al., *Cellular uptake of nanoparticles: journey inside the cell.* Chemical Society Reviews, 2017. **46**(14): p. 4218-4244.
106. Zhang, J.-M. and J. An, *Cytokines, Inflammation, and Pain.* International Anesthesiology Clinics, 2007. **45**(2): p. 27-37.
107. Hu, M. and D. Palić, *Micro- and nano-plastics activation of oxidative and inflammatory adverse outcome pathways.* Redox Biology, 2020. **37**: p. 101620.
108. Rahman, M.M. and G. McFadden, *Modulation of NF-κB signalling by microbial pathogens.* Nature Reviews Microbiology, 2011. **9**(4): p. 291-306.
109. Syed, S., A. Zubair, and M. Frieri, *Immune Response to Nanomaterials: Implications for Medicine and Literature Review.* Current Allergy and Asthma Reports, 2013. **13**(1): p. 50-57.
110. Akisue, T., et al., *The effect of particle wear debris on NFkappaB activation and pro-inflammatory cytokine release in differentiated THP-1 cells.* J Biomed Mater Res, 2002. **59**(3): p. 507-15.
111. Fuchs, A.K., et al., *Carboxyl- and amino-functionalized polystyrene nanoparticles differentially affect the polarization profile of M1 and M2 macrophage subsets.* Biomaterials, 2016. **85**: p. 78-87.
112. Bosshart, H. and M. Heinzelmann, *THP-1 cells as a model for human monocytes.* Annals of translational medicine, 2016. **4**(21): p. 438-438.
113. Schutte, R.J., A. Parisi-Amon, and W.M. Reichert, *Cytokine profiling using monocytes/macrophages cultured on common biomaterials with a range of surface chemistries.* Journal of biomedical materials research. Part A, 2009. **88**(1): p. 128-139.
114. Grosse, S., J. Stenvik, and A.M. Nilsen, *Iron oxide nanoparticles modulate lipopolysaccharide-induced inflammatory responses in primary human monocytes.* Int J Nanomedicine, 2016. **11**: p. 4625-4642.
115. Rehman, M.U., et al., *The anti-inflammatory effects of platinum nanoparticles on the lipopolysaccharide-induced inflammatory response in RAW 264.7 macrophages.* Inflamm Res, 2012. **61**(11): p. 1177-85.

Appendix A: Equipment and reagents

Table A.1 List of equipment and reagents used and the vendor from which they were acquired, and the corresponding catalogue number.

Reagents	Vendor	Catalogue number
Cell cultivation		
RPMI-1640 medium	Sigma-Aldrich	R0883
Fetal bovine serum	Sigma-Aldrich	F7524
L-Glutamine	Sigma-Aldrich	G8540
Gentamicin	Sigma Aldrich	G1397
Corning 75 cm^2 Cell culture flask	Sigma-Aldrich	CLS430641U
Phosphate Buffered Saline Tablets	Sigma-Aldrich	P4417
RNA extraction		
β-mercaptoethanol	Sigma-Aldrich	M7522
E.Z.N.A.® Total RNA Kit I	Omega BIO-TEK	R6834-02
RNeasy® Mini Kit (250)	Qiagen	74106
QuantiTect® Reverse Transcription Kit (200)	Qiagen	205313
Differentiation reagents		
Phorbol 12-myristate 13-acetate (PMA)	Sigma-Aldrich	P8139-5MG
Interferon gamma (IFNγ)	Sigma-Aldrich	11040596001
Lipopolysaccharide (LPS)	Sigma-Aldrich	L2654-1MG
Staining dyes and Antibodies		
CellMask™ Deep Red Plasma Membrane Stain	Thermo-fisher	C10446
Adipored	Lonza	PT-7009
DAPI	Invitrogen	D1306
NF-κB p65 (L8F6) Mouse Ab	Cell Signalling Technology	6956S
AlexaFluor™ 546 goat anti-mouse IgG (H+L)	Invitrogen	A11030
AlexaFluor™ 594 goat anti-mouse IgG (H+L)	Invitrogen	A11032
cDNA synthesis		
QuantiTect® Reverse Transcription Kit (200)	Qiagen	205313
qPCR		
LightCycler® 480 Multiwell Plate 96	Roche	04729692001
LightCycler® 480 SYBR® Green I Master	Roche	04887352001
Resazurin assay		
Resazurin	R&D Systems	AR002

ELISA

Human TNFα DuoSet	R&D Systems	DY210-05
Human IL-6 DuoSet	R&D Systems	DY206-05
Human IL-10 DuoSet	R&D Systems	DY217B-05
DuoSet ELISA Ancillary Reagent Kit 2	R&D Systems	DY008

Appendix B: Characterization of NMP's by NTA and CLSM

Table B.1. Settings of nano tracking analysis for the particle stock suspensions

Suspension	Dilution Factor	Camera Level	Temperature	Measurement Time	Detection Threshold	Blur	Jump Distance	Min. Track Length
PMMA	1:100	14	37°C	120s	8	5×5	12	10
Control for PMMA	1:100	14	37°C	120s	8	5×5	12	10
PS	1:100	12	37°C	120s	8	5×5	12	10
Control for PS	1:100	12	37°C	120s	8	5×5	12	10
PVC	1:1000	12	37°C	120s	10	5×5	12	10
Control for PVC	1:1000	12	37°C	120s	10	5×5	12	10

Table B.2. Laser settings used for visualization of the NMP's in CLSM

NMP's	Laser
PMMA	488nm
PS	561 nm
PVC (NileRed)	561 nm

Appendix C: Additional data from TBT4500 course – Time-dependent relative expression of differentiation markers

In this experiment, the cells were treated with 10 nM PMA for 4 h, 24 h, and 48 h. *CD36* induction was seen at 24 hours, whereas *CD14* induction peaked at 48 hours. Thus, the results demonstrated that the monocytes were differentiated into macrophages with PMA treatment.

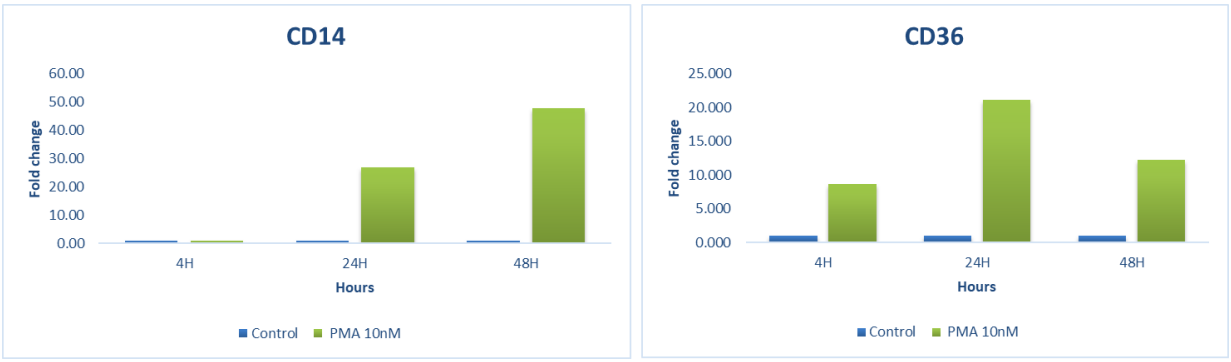

Figure C.1. qPCR analysis of *CD14* and *CD36* gene markers in PMA-differentiated macrophages along the indicated time-point. The results are obtained from a single experiment (n=1)

Appendix D: Gene expression analysis by qPCR

Table D.1. Temperature conditions in the LightCycler

Step	Temperature	Time	Cycles
Pre-incubation	95°C	10 min	1
Amplification			45
Denaturation	95°C	10 sec	
Annealing	55°C	10 sec	
Extending	72°C	10 sec	
Melting	95°C	5 sec	1
	65°C	60 sec	
	97°C	1 sec	
Cooling	40°C	10 sec	1

Table D.2. List of primers used and their sequences.

Gene	Sequence
Human ACTB	forward 5´- AAGACCTCTATGCCAACAC -3´ reverse 5´- TGATCTTCATGGTGCTAGG -3´
Human RPS18	forward 5´- CAGAAGGATGTAAAGGATGG-3´ reverse 5´-TATTTCTTCTTGGACACACC-3´
Human GAPDH	forward 5´-ACAGTTGCCATGGTAGACC-3´ reverse 5´-TTTTTGGTTGAGCACAGG-3´
Human CCL2	forward 5´- AGACTAACCCAGAAACATCC -3´ reverse 5´- ATTGATTGCATCTGGCTG -3´
Human TNFα	forward 5´- AGGCAGTCAGATCATCTTC -3´ reverse 5´-TTATCTCTCAGCTCCACG -3´
Human IL-12	forward 5´-AAGACCTCTTTTATGATGGC -3´ reverse 5´-CATTCATGGTCTTGAACTCC -3´
Human COX-2	forward 5´- AAGCAGGCTAATACTGATAGG -3´ reverse 5´-TGTTGAAAAGTAGTTCTGGG -3´
Human IL-6	forward 5´- GCAGAAAAAGGCAAAGAAT -3´ reverse 5´- CTACATTTGCCGAAGAGC -3´
Human SOCS3	forward 5´- CCTATTACATCTACTCCGGG -3´ reverse 5´- ACTTTCTCATAGGAGTCCAG -3´
Human IL-1β	forward 5´- CTAAACAGATGAAGTGCTCC -3´ reverse 5´- GGTCATTCTCCTGGAAGG -3´
Human RelA	forward 5´- GAAGAAAAACGCAAAAGAAC -3´ reverse 5´- TTCAGTTGGTCCATTGAAAG -3´

Appendix E: Additional data – Uptake studies of NMP's in macrophages

For this experiment, macrophages were exposed to the different NMP's for 30 min, 2 h, and 16 h. After treatment, the cells were fixed and stained with the plasma membrane and Hoechst stain for visualizing the nuclei and cell membrane. The fixed cells were imaged using confocal microscopy with a 63x/1.4 oil immersion. Z-stacks were performed for determining the internalization of the NMP's. For PVC, we stained the particles with NileRed after fixing the treated cells.

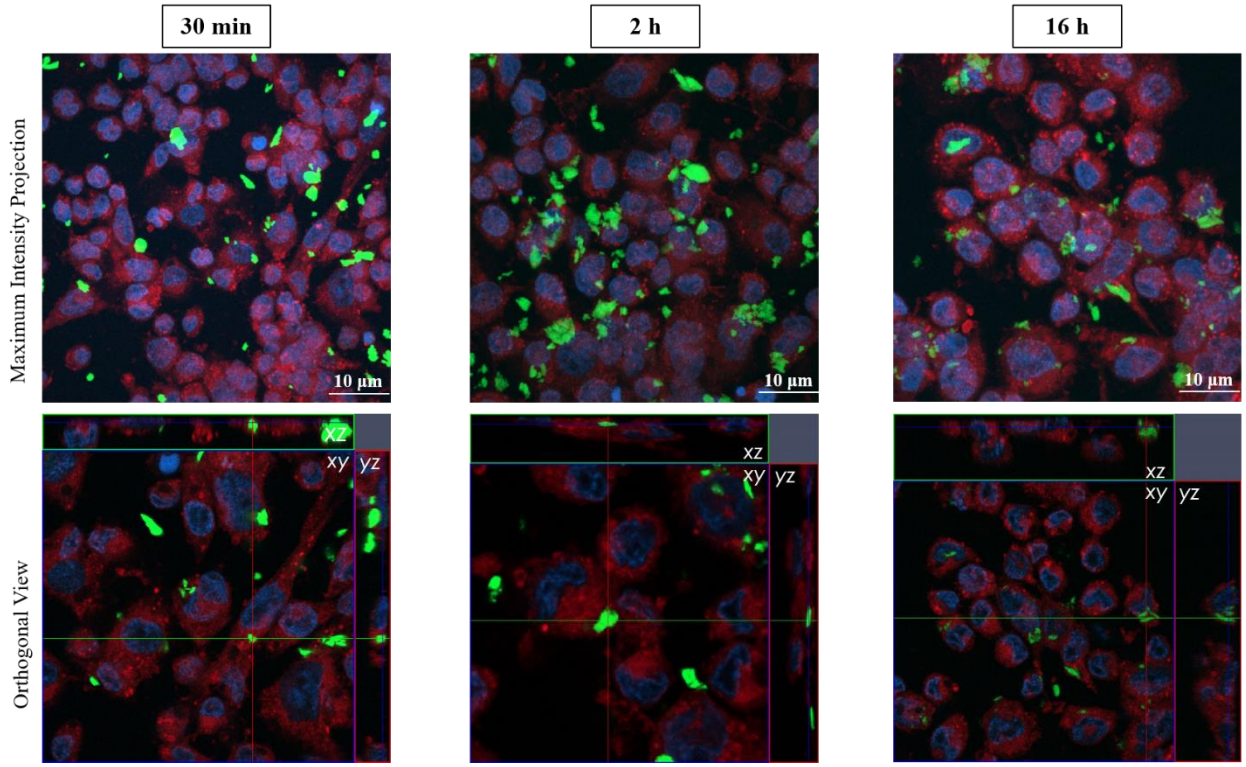

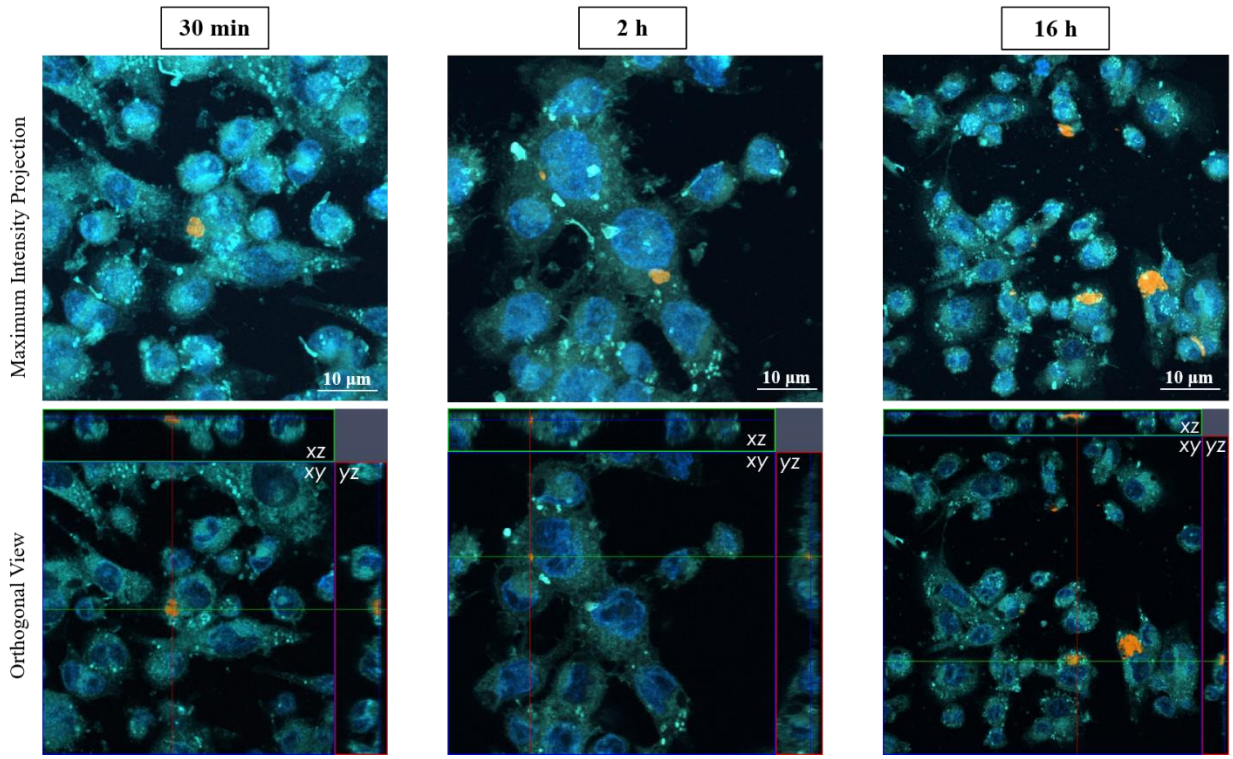

Figure E.1. Representative images showing the internalization of NMP's in THP-1 derived macrophages. Macrophages were exposed to **PMMA** and **PS** for indicated time points. The images presented here show the maximum intensity projection view of images obtained from the Z-stack series and the orthogonal view (x-y projection along with respective side views (x-z and y-z projections)).

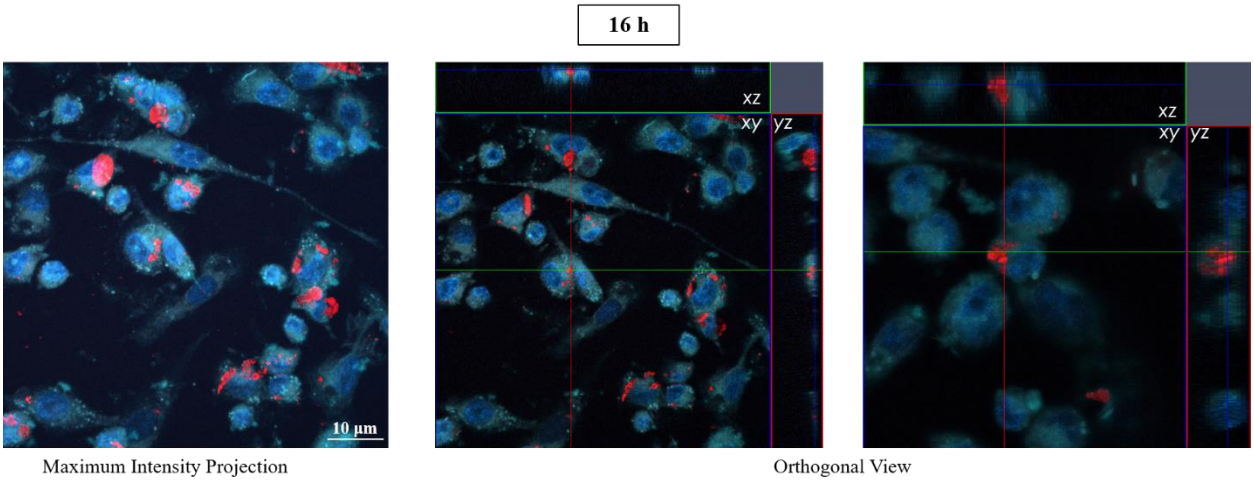

Figure E.2. Representative images showing the internalization of Nile Red stained PVC in THP-1 derived macrophages. Macrophages were exposed to PVC for 16 h. The images presented here show the maximum intensity projection view of images obtained from the Z-stack series and the orthogonal view (x-y projection along with respective side views (x-z and y-z projections)).

Appendix F: Additional data – Relative expression of M1 markers in NMP's exposed macrophages

THP-1 derived macrophages were exposed to PMMA, PS and PVC for 48 h and 72 h. Total RNA was analyzed for expression of *CCL2* and *IL-12* using qPCR. The gene expression analysis was not performed for the positive control.

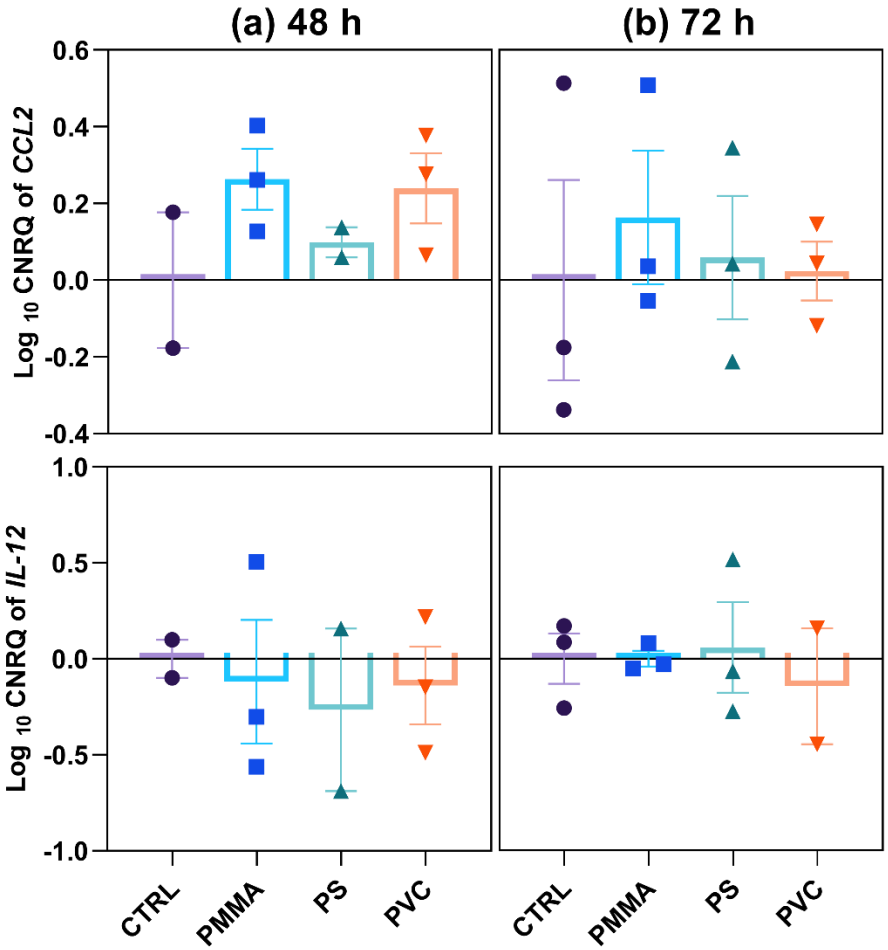

Figure F.1. Relative expression of M1 macrophage marker genes in macrophages exposed to NMP's. THP-1 derived macrophages were exposed vehicle (CTRL) or to PMMA, PS, or PVC at the highest particle concentrations for the indicated time points. Graphs show the relative gene expression of *CCL2* and *IL-12* at **(a)** 48 h and **(b)** 72 h. measured using qPCR. Data were normalized to three reference genes, and the mean expression relative to the vehicle-treated control (CTRL) (CNRQ) ± SEM is shown. Data for the NMP's exposures represent the results from three independent experiments (n=3.), no positive control was kept during the experiment. Statistical analysis was carried out with one-way ANOVA in qbase+.

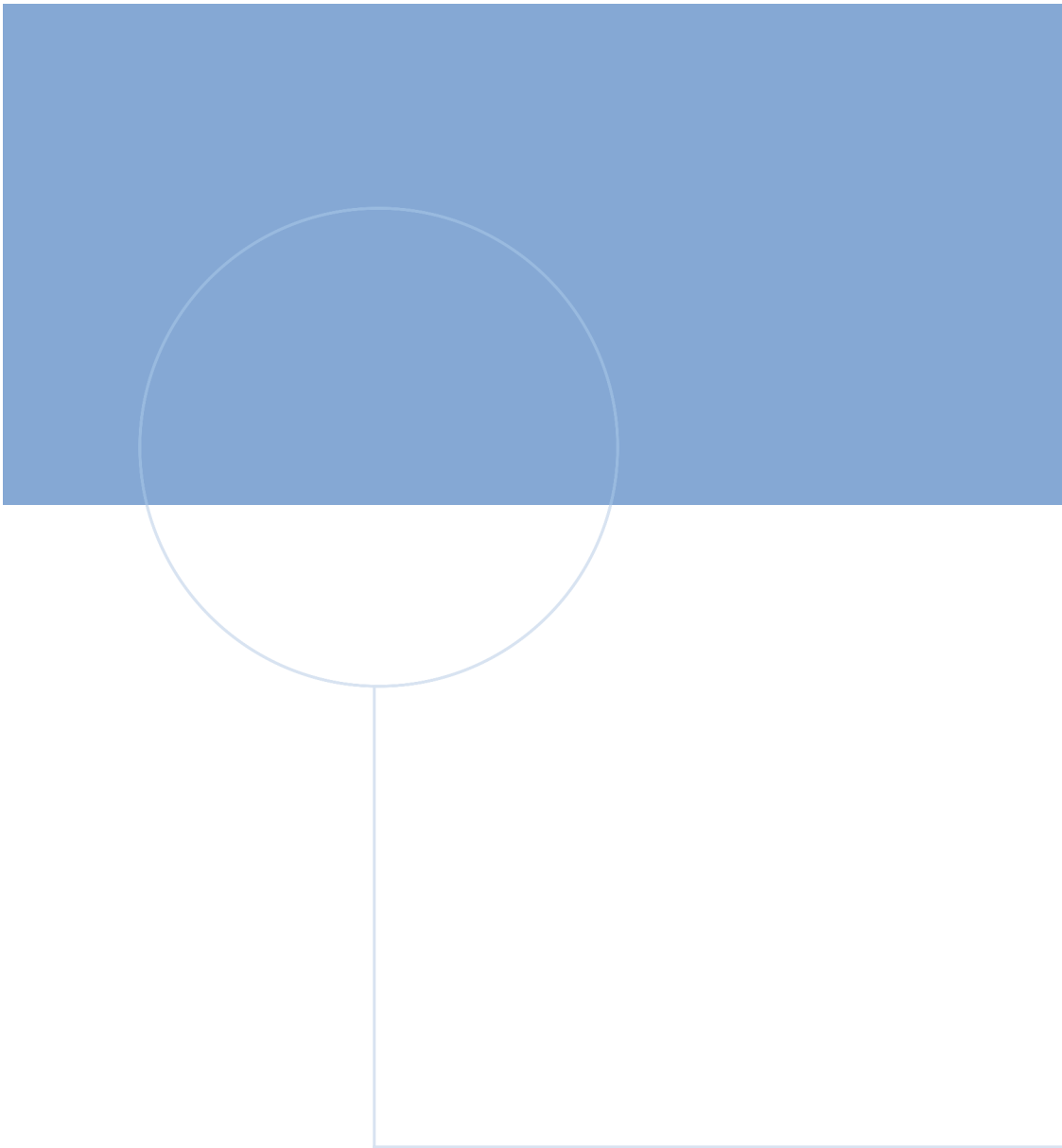

NTNU

Norwegian University of
Science and Technology